Quaternary Science Reviews 141 (2016) 38–51

Contents lists available at ScienceDirect

Quaternary Science Reviews

journal homepage: www.elsevier.com/locate/quascirev

The structure of Holocene climate change in mid-latitude North America

Bryan N. Shuman*, Jeremiah Marsicek

Department of Geology & Geophysics, Roy J. Shlemon Center for Quaternary Studies, University of Wyoming, 1000 E. University Ave, Laramie WY 82070, USA

ARTICLE INFO

Article history:
Received 11 November 2014
Received in revised form
2 March 2016
Accepted 8 March 2016

Keywords:
Climate change
Temperature
Precipitation
Abrupt change
Holocene
North America

ABSTRACT

A sequence of long-term and rapid changes during the Holocene appears in a network of 40 well-resolved paleoclimate datasets from mid-latitude North America, including records of pollen-inferred temperatures, alkenone-derived sea-surface temperatures (SSTs), lake-level changes, dust accumulation, and lake isotopes from Idaho to Maine. Statistical analyses reveal that changes in insolation and the Laurentide Ice Sheet explain 51.7% of the variance in the records, especially multi-millennial trends, but peak rates of change indicate additional rapid changes at ca. 10.8, 9.4, 8.3, 7.0, 5.5–5.2, 4.7, 2.1, and 0.9 ka. Step changes between 9.4 and 8.3 ka relate to ice sheet dynamics that warmed much of the region, and changes at 5.5 ka were the largest since the demise of the ice sheet. The shift at 5.5 ka initiated widespread cooling and increases in effective moisture, which culminated in the coolest, wettest millennia in most areas after 2.1 ka. Replicated evidence from multiple records also shows a spatially-varied set of multi-century fluctuations including 1) low temperatures and high effective moisture at 5.5–4.8 ka in the mid-continent and 2) repeated phases of low SSTs, cool summers, and drought superimposed upon long cooling, moistening trends in eastern North American since 5.5 ka.

1. Introduction

Efforts to understand Holocene climate change have demonstrated the importance of insolation, ice sheet, and greenhouse gas changes at multi-millennial scales (e.g., COHMAP, 1988; Kaufman et al., 2004; Liu et al., 2014; Marcott et al., 2013; Renssen et al., 2009), but millennial-to-centennial variations and events also shaped Holocene climates (Alley et al., 1997; Booth et al., 2005; deMenocal et al., 2000; Fleitmann et al., 2008; Magny and Haas, 2004; Magny et al., 2006; Martin-Puertas et al., 2012; Neff et al., 2001; van Geel et al., 2000). Changes composed smooth temporal trends when averaged at global-to-continental scales (Marcott et al., 2013), but long waves in the westerlies guarantee that many mid-latitude changes were expressed as mosaics of regional anomalies of different sign and magnitude (Donders et al., 2008; Morrill et al., 2013; Renssen et al., 2009) and with different multivariate characteristics (Morrill et al., 2013; Rach et al., 2014). Diagnosing the full spectrum of Holocene climate changes, therefore, requires comparisons of many complementary paleoclimate records (Mayewski et al., 2004; Wanner et al., 2011, 2008).

In mid-latitude North America, Holocene climate history differed from that of other regions because of a specific combination of long-term trends (e.g., Bartlein et al., 2011; Viau et al., 2006), regime shifts (Shuman et al., 2002; Williams et al., 2010), and variability at annual to multi-centennial scales (Booth et al., 2006; Grimm et al., 2011; Nelson et al., 2011; Newby et al., 2014; Nichols and Huang, 2012). Here, we attempt to integrate multiple temperature, moisture, and isotopic records to describe the most coherent and robust Holocene paleoclimate signals. We use a network of 40 records to document the relative sequence and covariance, i.e., the structure, of temperature and moisture trends, steps, and events from the Rocky Mountains to the Atlantic coast (Fig. 1). We define trends as progressive, multi-millennial changes; steps as non-reversing changes that took place within centuries; and events as temporary (reversing) fluctuations that lasted less than ~1000 years.

Individual datasets cannot detect all regionally-significant changes because any given change may be spatially heterogeneous and may not affect all sites (Cook and Krusic, 2004; Mann et al., 2009; Williams et al., 2010). Likewise, individual parameters (e.g., temperature or drought severity) cannot represent the

* Corresponding author.
E-mail address: bshuman@uwyo.edu (B.N. Shuman).

http://dx.doi.org/10.1016/j.quascirev.2016.03.009
0277-3791/

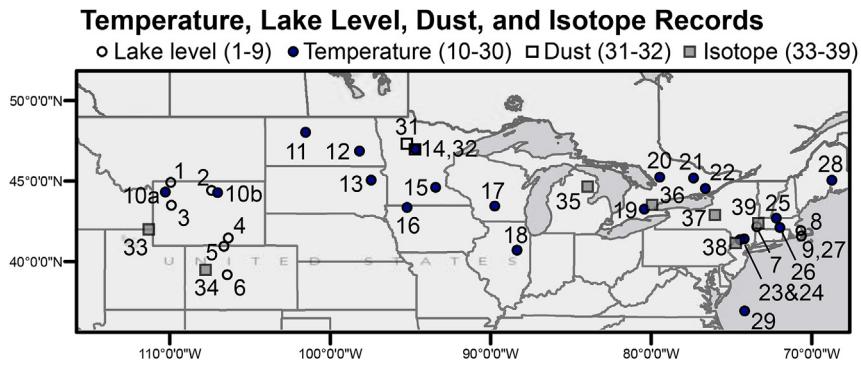

Fig. 1. A map of the North American paleoclimate records used here. Numbers correspond with those in Table 1.

full complexity of the climate history (Rach et al., 2014). For these reasons, we follow Alley's (2003) suggestion to use multiply-replicated, multi-parameter analyses as a way to improve reliability and confidence in the paleoclimate signals. We focus on four types of records that have been consistently measured at multiple locations and that can be readily interpreted as representing key climate variables. In particular, we use the multi-site, multi-record evidence to evaluate when and where steps and events punctuated the well-documented long trends.

To do so, we produce regional and sub-regional averages (stacks) of 1) pollen- and alkenone-inferred summer temperatures; 2) quantified lake-level changes; 3) relative dust accumulation rates; and 4) lake-sediment isotopic values. We use the regional and sub-regional means of each data type to filter local ecological, hydrological, or geochemical factors and to clarify common climate signals that extend beyond individual sites. Correlations among variables further confirm where and when important climate signals have been detected by multiple independent approaches. We calculate rates of change and use principal components to identify common periods and patterns of changes. The relative significance and sequences of change can help to diagnose the North American climate dynamics that were important for ecological, geomorphic, and cultural changes during the Holocene (e.g., Foster et al., 2006; Halfen and Johnson, 2013; Kelly et al., 2013; Munoz et al., 2011).

2. Methods

2.1. Data

Our analysis uses a network of 40 records from 38 sites between the Rocky Mountains (Colorado, Wyoming, Idaho) and the North Atlantic coast (including two marine records from off Virginia and Nova Scotia). They represent the region influenced by Atlantic-derived moisture and air masses in mid-latitude North America, and span the west-to-east North American moisture gradient (Bryson, 1966; Liu et al., 2010). Annual temperatures vary little across the region today, but seasonal temperature differences decline and annual precipitation increases from <400 mm to >1100 mm from west to east (NCDC, 1994). Mean July temperatures do not vary systematically by longitude within the study area, but range from 18 °C at the northern sites to 24 °C in the south (NCDC, 1994).

Most records were either generated by us or were publically available (Fig. 1; Table 1). Each was required to have spanned from <0.6 to >10.0 ka for the purpose of consistent statistical power throughout the Holocene, and as a result, we excluded some relevant and well-resolved isotope datasets that did not extend to before 9 ka (e.g., Anderson, 2012; Smith et al., 2002). To evaluate sub-regional differences, we divided the datasets into four sub-regions: western (Colorado to North Dakota); west-central (South Dakota to Illinois); east-central (Ontario); and eastern (New York to Maine). Groupings were predominantly geographical, but were modified based on clusters of records identified using principal components analyses (see Section 2.2).

2.1.1. Temperature records

Of the 40 records, nineteen document changes in the mean temperature of the warmest month (MTWM). The MTWM records derive from well-resolved pollen-inferred reconstructions (>70 samples/11,000 years) from North Dakota to Maine (Table 1), and are supplemented by a temperature reconstruction based on two pollen records from northern Wyoming (Kelly et al., 2013; Shuman, 2012a) to extend the geographic coverage. We focus on regional averages of the reconstructions because they represent the common temperature signals and average out local ecological influences (e.g., local disturbances), but we also discuss where individual records either deviate from or provide support for the mean patterns.

The reconstructions were generated using a widely applied space-for-time substitution (modern analog) technique (Overpeck et al., 1985), which assigned temperatures to each fossil sample based on comparisons with >4000 modern pollen samples from across North America (Whitmore et al., 2005). We followed methodological suggestions from Williams and Shuman (2008) including a) averaging the MTWM values from the seven best modern analogs for each sample, b) using 64 regionally-split taxa for the comparisons, and c) applying the squared chord distance as the measure of comparison. We place the MTWM reconstructions in the context of other paleoenvironmental records to assess the coherency of the climate signals and the nature of moisture and isotopic changes that coincided with the regional temperature changes.

As an additional comparison and to further extend the geographic coverage of temperature records, we also include two sea-surface temperature (SST) reconstructions derived from alkenone paleothermometry from the margin of eastern mid-latitude North America (Sachs, 2007). We linearly detrended (and evaluate the detrending of) the original temperature series, however, because the raw SST reconstructions contain a large magnitude trend that indicates that late-Pleistocene (Younger Dryas) temperatures were 5 °C greater than today (Sachs, 2007) and that may have resulted from nutrient, light, seasonality, or depth biases in alkenone production (Kim et al., 2004; Prahl et al., 2006). At a minimum, the large trends were not likely representative of conditions on the continent where late-Pleistocene cold is well documented (Levesque et al., 1997; Mott et al., 1986; Peteet et al., 1990),

Table 1
Site Table. "MTWM" refers to mean temperature of the warmest month; "SST" to sea-surface temperatures; "18O" to oxygen isotope records; and "2H" to hydrogen isotope records.

Number	Site	State/ Province	Latitude	Longitude	^{14}C dates	Samples	Temperature	Lake level	Isotope	Dust	Pollen citation	Citation for reconstruction
1	Rainbow Lake	WY	44.94	−109.50	29	220		X				Shuman and Serravezza, unpub.
2	Lower Paintrock Lake	WY	44.39	−107.38	39	220		X				Serravezza and Shuman, unpub.
3	Lake of the Woods	WY	43.48	−109.89	21	220		X				Pribyl and Shuman (2014)
4	Little Windy Hill Pond	WY	41.43	−106.33	18	220		X				Minckley et al. (2012)
5	Upper Big Creek Lake	CO	40.91	−106.62	7	220		X				Shuman et al.(2015)
6	Emerald Lake	CO	39.15	−106.41	29	220		X				Shuman et al. (2014)
7	Davis Pond	MA	42.14	−73.41	31	220		X				Newby et al. (2011, 2014)
8	New Long Pond	MA	41.85	−70.68	52	220		X				Newby et al. (2009, 2014)
9, 27	Deep Pond	MA	41.56	−70.64	53	125/220	MTWM	X			Foster et al. (2006)	Marsicek et al. (2013)
10a	Buckbean Bog	WY	44.30	−110.26	4	45	MTWM				Baker (1976)	Shuman (2012)
10b	Sherd Lake	WY	44.27	−107.01	2	48	MTWM				Burkart (1976)	Shuman (2012)
11	Rice Lake	ND	48.01	−101.53	14	81	MTWM				Grimm (2001)	This study
12	Moon Lake	ND	46.86	−98.16	14	144	MTWM				Laird et al. (1996)	This study
13	Pickerel Lake	SD	45.50	−97.33	3	73	MTWM				Watts and Bright (1968)	This study
14, 32	Steel Lake	MN	46.97	−94.68	35	119	MTWM			X	Wright et al. (2004)	This study
15	Sharkey Lake	MN	44.59	−93.41	9	163	MTWM				Camill et al. (2003)	This study
16	Lake West Okoboji	IA	43.33	−95.20	9	93	MTWM				Van Zant (1979)	This study
17	Devils Lake	WI	43.42	−89.73	12	98	MTWM				Baker et al. (1992)	This study
18	Chatsworth Bog	IL	40.68	−88.34	9	*55*	MTWM				King (1981)	This study
19	Nutt Lake	ON	45.22	−79.45	10	83	MTWM				Bennett (1983)	This study
20	Hams Lake	ON	43.24	−80.41	10	80	MTWM				Bennett (1983)	This study
21	Graham Lake	ON	45.18	−77.35	6	207	MTWM				Fuller (1998)	This study
22	High Lake	ON	44.52	−76.60	8	189	MTWM				Fuller (1998)	This study
23	Spruce Pond	NY	41.24	−74.20	9	141	MTWM				Maenza-Gmelch (1997)	This study
24	Sutherland Pond	NY	41.39	−74.20	11	140	MTWM				Maenza-Gmelch (1997)	This study
25	Little Pond-Royalston	MA	42.68	−72.19	7	83	MTWM				Oswald et al. (2007)	Marsicek et al. (2013)
26	Blood Pond	MA	42.08	−71.96	15	125	MTWM				Oswald et al. (2007)	Marsicek et al. (2013)
28	Mansell Pond	ME	45.04	−68.73	10	110	MTWM				Almquist-Jacobson and Sanger (1995)	This study
29	OCE326-GGC30	(Nova Scotia)	44.00	−63.00	8	141	SST					Sachs (2007)
30	CH0798 GGC19	(Virginia)	36.87	−74.57	5	165	SST					Sachs (2007)
31	Elk Lake	MN	45.87	−95.80	Varves	162				X		Dean (1997)
33	Bear Lake (cores 96-1/96-2)	UT/ID	41.98	−111.33	34	157			18O			Bright et al. (2006)
34	Bison Lake	CO	39.77	−107.35	9	284			18O			Anderson (2011)
35	O'Brien Lake	MI	44.64	−83.88	16	66			18O			Henne and Hu (2010)
36	Crawford Pond	ON	43.47	−79.95	4	73			18O			Yu et al. (1997)
37	Fayetteville Green Lake	NY	43.03	−75.97	6	998			18O			Kirby et al. (2002)
38	Grinnell Pond	NJ	41.10	−74.63	7	334			18O			Zhao et al. (2010)
39	Berry Pond	MA	42.51	−73.32	16	35			2H			Shuman et al. (2006)

but the additional variability may be relevant and is, therefore, evaluated here.

2.1.2. Moisture records

Nine records provide quantified estimates of Holocene lake-level changes. Several of the records from closed basin lakes have been used with mass-balance approaches to quantify precipitation minus evapotranspiration (P-E) through time (Marsicek et al., 2013; Newby et al., 2014; Pribyl and Shuman, 2014; Shuman et al., 2010), but P-E cannot be easily produced for overflowing lakes (i.e., Upper Big Creek and Lower Paintrock Lakes in Colorado and Wyoming, Table 1) or for the two other effective moisture records used here (relative dust accumulation rates from Elk and Steel Lakes, Minnesota). Therefore, and because the P-E reconstructions are simply linear transformations of the lake-level histories (Pribyl and Shuman, 2014), we transform all of the moisture records to z-scores. Z-scores measure deviations from the Holocene mean of each record in terms of standard deviations, and account for the different units in lake and dust records as well as the different magnitudes of water level change in lakes and watersheds of different sizes.

The lake-level reconstructions all rely on the same technique (Digerfeldt, 1986; Pribyl and Shuman, 2014), which uses transects of sediment cores and on-shore sediment profiles (supplemented with geophysical surveys) to track the elevation and lateral position of near-shore sediments as a direct measure of shoreline position. At each lake, sediment characteristics from 2 to 5 radiocarbon-dated cores from different water depths were systematically analyzed using a decision-tree approach applied in R (R Core Development Team, 2009) to determine intervals containing near-shore sediments (paleoshoreline deposits). Water-level changes were then reconstructed systematically in R based on the

changing elevations of the near-shore sediments at each site (Pribyl and Shuman, 2014).

The two lake-sediment mineralogy datasets from Minnesota (Dean, 1997; Nelson and Hu, 2008) provide an index of aeolian dust accumulation based on the sediment fraction of fine quartz and feldspars measured by x-ray diffraction (XRD). Aeolian dust accumulation likely reflects regional aridity because low effective moisture (P-E) reduces vegetation cover and facilitates aeolian erosion (Forman et al., 2001; Kohfeld and Harrison, 2000). Because dust flux can relate to aridity in a non-linear fashion (e.g., potential dust-source areas may change exponentially in extent during drought) and because the data are not normally distributed, we log transformed the XRD data for all plots and analyses. Despite potential complexities, such as the role of winds and changing sources of fine particulates (Mason et al., 2003; McKean et al., 2015; Muhs et al., 2008), we use the records because they provide an opportunity to evaluate the fidelity of the signals in replicated records from the same area. They also provide detailed information about the relative sequence of hydroclimate changes in a sub-region without the type of quantitative lake level records used elsewhere.

2.1.3. Stable hydrogen and oxygen records

We compare the temperature and moisture records with seven stable hydrogen and oxygen isotope datasets from lake sediments, which are distributed across our four sub-regions. Six stable isotope datasets (Bear, Bison, O'Brien, Crawford, Fayetteville Green, and Grinnell lakes) represent the oxygen isotope composition of bulk carbonate sediments (Anderson, 2011; Bright et al., 2006; Henne and Hu, 2010; Kirby et al., 2002; Yu et al., 1997; Zhao et al., 2010), whereas one (Berry Pond) represents the hydrogen isotopic composition of C_{22} *n*-acid, an organic compound primarily derived from emergent aquatic plants (Hou et al., 2007; Shuman et al., 2006). Many interacting hemispheric to local scale processes can influence individual lake-sediment stable isotopes (Gibson and Edwards, 2002; Gibson et al., 2002; Henderson and Shuman, 2009; Jasechko et al., 2013; LeGrande and Schmidt, 2009; Schlaepfer et al., 2014; Smith and Hollander, 1999; Steinman and Abbott, 2013), but networks of lakes can retain important patterns related to climate and atmospheric circulation (e.g., Henderson and Shuman, 2009; Shanahan et al., 2015). As with the other types of records, our comparisons reveal the regional fidelity of the embedded signals.

2.2. Analyses

Regional and sub-regional mean temperature and moisture histories were calculated where multiple records could be averaged. We plot standard errors to show the confidence in the mean patterns of change, but also assess the signals in combinations of records by generating means for all factorial combinations of the individual datasets. Doing so reveals the sensitivity of the mean record to inclusion of any individual record and its particular age uncertainties, sample spacing, and reconstruction errors. Likewise, we completed 100 bootstrapped iterations of principal components analysis (PCA) in R to quantify the amount of variance common across 1) all datasets and 2) three categories of data: temperature, effective moisture (lake-level and dust accumulation), and isotope records. To do so, we randomly selected (with replacement) from the relevant pool of records to generate 100 random combinations of records equal to the original number used for PCA. We conducted the PCA on correlation matrices except when analyzing temperatures alone. For temperature, the covariance matrix was used to retain the magnitude of the signals in degrees C. We also used the PCA loadings to identify regional groups of correlated datasets and to recognize outliers before calculating regional means of the different variables.

We defined abrupt changes as times when the rates of change over 200 year intervals rose above 85% of the background rates. We computed the rates of change in terms of the absolute change in z-scores from the beginning to end of each 200-year interval. Mean rates were calculated for each data type, and then a mean of the data-type means was used as a summary index to avoid biases associated with differences in the number records of each data type. We focus on the periods of major abrupt changes identified in the summary index, but also use peaks in the rates of change from the different types of records, sub-regions, and principal components to identify periods of abrupt changes as expressed by these other metrics. For this reason, we provide different ages for some changes depending on the metric being discussed.

We also calculated correlations among records, regional and subregional means, and PCA scores to assess the coherency of the signals. We applied linear regression and Granger causality tests in R to further quantify the relationships. Linear models quantify the amount of variance in one time series that can be explained by another or by important forcing functions (i.e., time series of insolation and glacial extent) (Berger and Loutre, 1991; Dyke, 2004), but because autocorrelation within time series data can produce spurious correlations, we use the Granger tests to evaluate whether a given predictor provides more information than expected from autocorrelation alone (Granger, 1969).

To complete these analyses, all data were first interpolated to 50-yr time intervals in calendar years. We used published age models for the isotope, dust, and SST records, but developed age models for temperature and lake level records using *Bchron*, a Bayesian tool for incorporating calibrated radiocarbon uncertainties and sample spacing into age models (Haslett and Parnell, 2008; Parnell et al., 2008). Doing so enabled us to include updated chronological information for some of the sites (Grimm et al., 2009).

3. Results

3.1. Major patterns of temperature, moisture, and isotopic change

3.1.1. Mean regional changes

The record of regional mean temperatures (derived from pollen and alkenones) and effective moisture (from lake level and dust flux) confirms that the Holocene climate history of mid-latitude North America included a combination of long-term trends, abrupt shifts, and multi-century events (Fig. 2). Mean temperatures of the warmest month for the region rose progressively by >1.5 °C to a maximum at 7 ka and have since declined by >0.5 °C (Fig. 2A). Mean effective moisture levels across the region, however, have only recently achieved their maximum based on Holocene-scale changes in lake levels and dust flux of >1.5 sd (Fig. 2B).

Prominent accelerations of the long-term trends decreased temperatures and increased effective moisture at 5.5–4.7 and 2.1–1.8 ka (Fig. 2). The multi-century changes equaled about 50% of the magnitude of the long-term trends since 7 ka, but were >140% as rapid. The mean rate of change across all datasets exceeded 85% of the rates (0.26 sd/200 yrs) seven times: at 10.9–10.5, 9.4, 8.3, 5.5, 5.2, 4.7, and 0.9–0.6 ka (Fig. 3, top panel). During these intervals, abrupt century-scale shifts in temperature and effective moisture (vertical dashed lines, Fig. 2) punctuated the progressive background trends, which had a mean background rate of change of 0.18 ± 0.09 sd/200 yr.

Several of the rapid changes cluster in the early Holocene (Figs. 2–4). Effective moisture and temperature increased rapidly by 10.5 ka, and then shifted stepwise at ca. 9.3–9.1 and 8.4–8.0 ka respectively. Effective moisture declined stepwise at 9.3–9.1 ka by

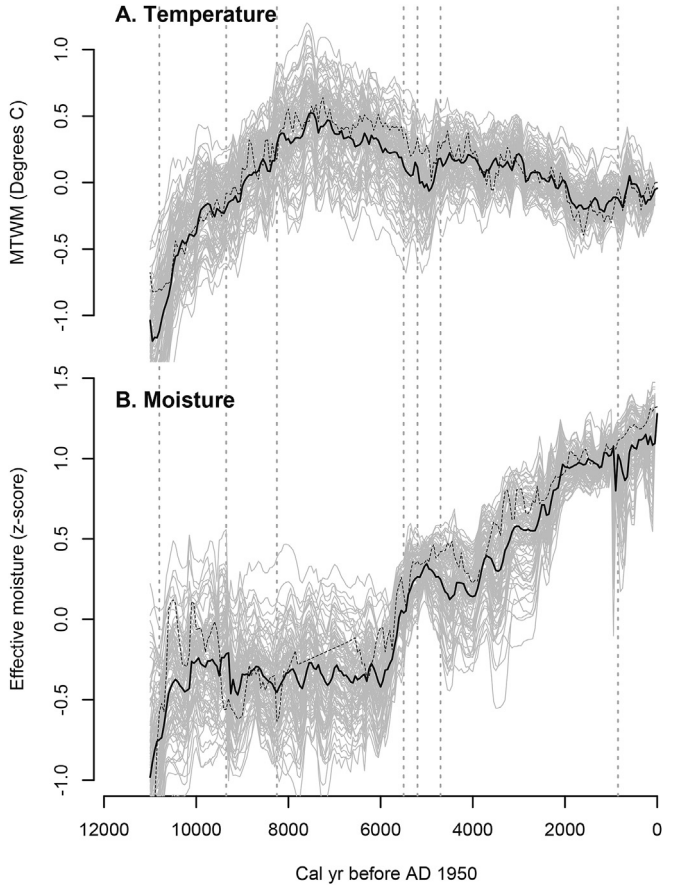

Fig. 2. A. Mean (solid black line) and median (dashed black line) of all of the pollen- and alkenone-inferred temperature time series from the region (black circles, Fig. 1). Gray lines shows each of the means from all possible factorial combinations of records. B. Mean (solid black line) and median (dashed black line) of all of the effective moisture (lake level and dust) records, plotted as z-scores. Gray lines show all possible factorial combinations. Vertical dashed lines indicate the timing of maxima in the mean rate of change across all data types (Fig. 3A).

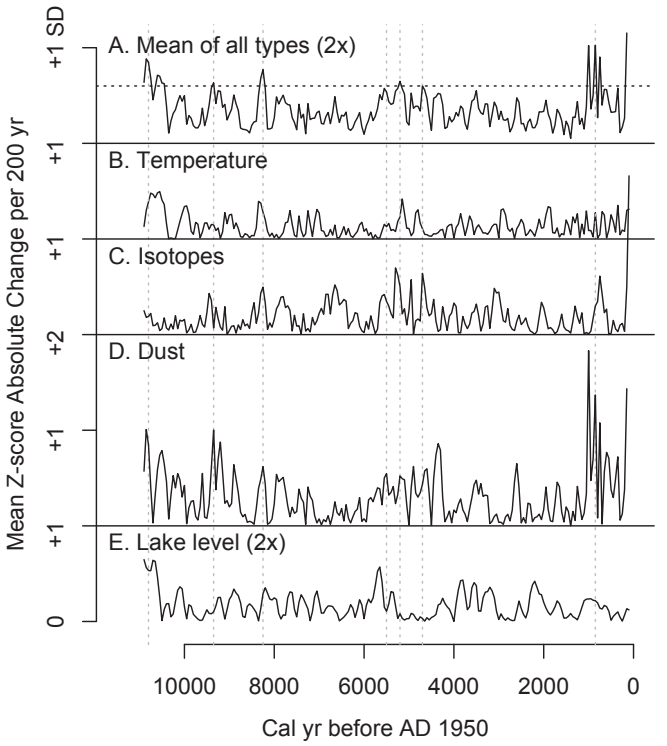

Fig. 3. Mean rates of change over 200-yr intervals plotted by data type compared with each other. Panel A represents the mean of all of the time series (B–E) below, which show the mean absolute magnitude of change in the various categories of data. The vertical scale indicates +1 z-score (standard deviation) units above each of the horizontal lines, which mark zero for the time series above. The horizontal dashed line in A marks the threshold for distinguishing major episodes of abrupt change (0.26 sd/200 yrs; 85% of the rates) at 10.9–10.5, 9.4, 8.3, 5.5, 5.2, 4.7, and 0.9–0.6 ka, which are also indicated by vertical dashed lines (as in Fig. 2). Peaks within 300 years of each other are treated as single events.

0.2 sd/200 yr, which is more than twice the mean background rate of lake-level change of 0.08 ± 0.07 sd/200 yr and especially prominent in the median of the moisture records (thin black line, Fig. 2B). The step change initiated a new multi-millennial mean that persisted until 6 ka (Fig. 2B). The second principal component of the moisture records emphasizes that the shift represents part of a large moisture change from 9.3 to 7.4 ka (Fig. 4B). Temperatures experienced a similar stepwise increase of 0.2 °C to a new multi-millennial mean at 8.4–8.0 ka (Fig. 2A). PCA confirms that temperature changes at 8.4–8.0 ka included both a cool event (Fig. 4A, lower panel) and a step change (Fig. 4A, upper panel).

The most prominent interval of anomalously low temperatures developed at 5.5–4.7 ka after the single largest and most coherent increase in effective moisture in the Holocene record (Figs. 2–4). The largest change in the ensemble of stable isotope records also took place at this time (Fig. 4C); PC1 of isotopic records contrasts the distribution of values before 5.2 ka with more recent values. PCA of the temperature records indicates, however, that the net regional cooling at 5.5–4.7 ka may be a combination of two different patterns: peak rates of cooling at many sites by 4.8 ka (Fig. 4A, top) as well as a brief cool event when temperatures were ~0.5 °C lower than the mid-Holocene mean for ca. 400 years from 5.2 to 4.8 ka (Fig. 4A, bottom). The highest mid-Holocene rates of mean regional temperature change bracketed this later event (Fig. 3B), and median temperatures reached two minima at 5.5–5.2 and 5.0–4.8 ka (thin black line, Fig 2A).

Warming combined with widespread drought at 4.7 ka to end the anomalously cool, wet conditions that began after 5.5 ka (Fig. 2). Afterwards, mean regional temperatures changed little until 2.9 ka, except for a minimum from 3.9 to 3.5 ka and a maximum at 3.0 ka; both events shifted the distribution of boot strapped temperatures (gray lines, Fig. 2A). The extensive drought after 4.7 ka persisted until 4.0 ka (with median moisture levels reaching a minimum from 4.2 to 3.9 ka), but the drought was followed by a progressive increase in effective moisture to present (Figs. 2B and 4B). Additional drought episodes at 3.6–3.3 and 3.0–2.4 ka had sufficient severity across records to also temporarily decrease the median and mean effective moisture z-scores relative to the long-term increase, but the events did not achieve the magnitude or extent of the aridity reconstructed at 4.7–4.0 ka (Fig. 2B).

Later shifts in both temperature (cooling) and effective moisture (increasing) at 2.6–1.8 ka represent a final acceleration of the long-term trends (Figs. 2 and 4), although they were not sufficiently rapid or synchronous to produce major peaks in the mean rates of change (>0.25 sd/200 yrs; Fig. 3). The transitions resulted in the establishment of modern-like conditions for the remainder of the Holocene, except for a prominent warm, dry episode from 0.80 to 0.35 ka (1150–1600 AD).

3.1.2. Common signals across variables

The temperature and moisture datasets share a significant

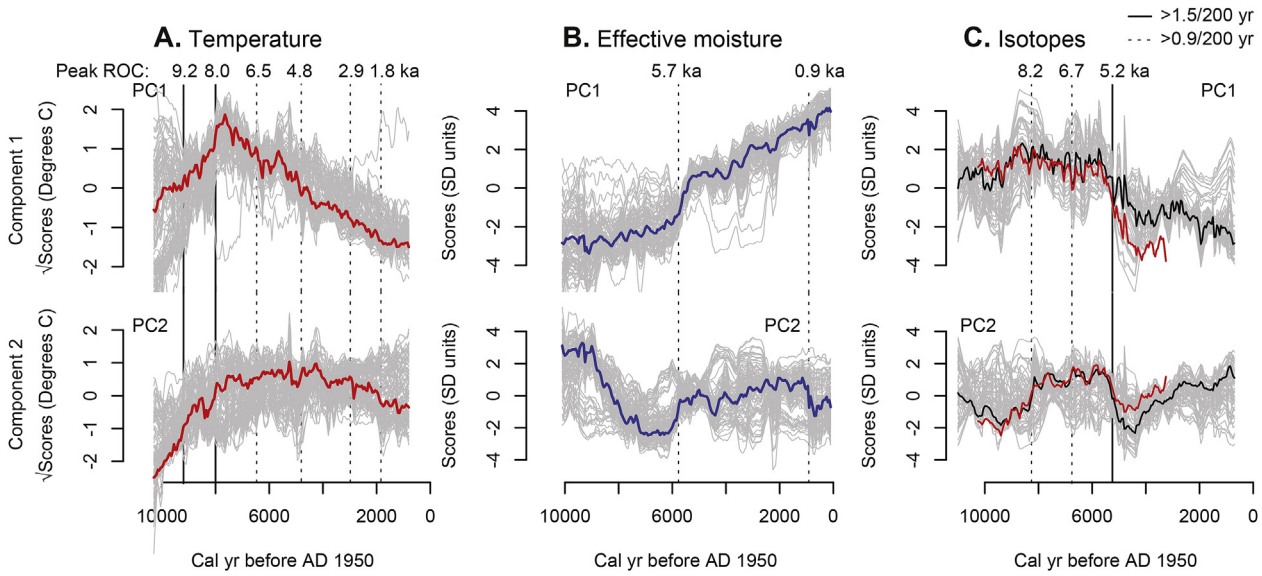

Fig. 4. First (top) and second (bottom) principal component (PC) scores plotted by time for A) all temperature reconstructions, B) all moisture reconstructions, and C) all isotope records. Thick lines indicate the scores based on PCA of all datasets, and gray lines indicate scores based on 100 iterations of the PCA using bootstrapped subsets of the data. Red lines in C represent a PCA that included two datasets (Fayetteville Green Lake and Bison Lake), which otherwise did not have sufficient duration for inclusion in our analyses. Vertical lines indicate maxima in the absolute magnitude of the rate of change in the component scores for each data type; solid lines indicate rates of >1.5 units per 200 years, and dashed lines indicate 0.9 units per 200 years. (For interpretation of the references to colour in this figure legend, the reader is referred to the web version of this article.)

amount of signal at multi-millennial to multi-century scales despite deriving from different types of records and from different sites. Over the last 7 ka, the mean regional temperature and moisture time series (Fig. 2) correlate significantly ($r = -0.90$; 1 sd range = −0.53 to −0.95). Granger causality tests indicate that each series contributes significantly more to predicting the other than autocorrelation within either series alone (moisture as a predictor of temperature: $F = 10.86$, $p = 0.0013$; temperature as a predictor of moisture: $F = 2.96$, $p = 0.087$). Rates of change confirm that departures from the long trends often influenced multiple variables simultaneously, although they also confirm differences among the sequences of moisture and temperature changes.

PCA of the entire multivariate dataset reveals that all four data types contribute similarly to the first three components, which explain >65% of the variance in the data (Table 2). The first component explains 34.9% of the variance (Fig. 5A), and the second explains an additional 21.0% (Fig. 5B). Together, they reveal two major long-term patterns: PC1 correlates ($r = 0.83$) with orbitally driven changes in seasonal insolation (red line, Fig. 5A) and PC2 correlates ($r = 0.91$) with the area of the Laurentide Ice Sheet (blue line, Fig. 5B). Removing the insolation trend from PC1 produces residuals that also correlate ($r = 0.97$) with the area of the ice sheet (gray line, Fig. 5B). Linear models show that insolation and ice sheet area explain 69.0% and 29.2% of the variance in PC1 respectively; ice sheet area explains 83.0% of PC2. Insolation and ice sheet area, therefore, explain at least 24.0% and 27.7%, respectively, of the total variance in our spatially distributed, multivariate dataset.

PC1 and PC2 also show a series of common features at multi-century scales (Fig. 5C–D). Both components include a stepwise deviation from the insolation and ice area trends at 9.3 ka, which was progressively reversed over the course of the Holocene by a long trend and a series of rapid steps and fluctuations of >0.5 sd at 8.4, 7.0, 5.3, and 2.1 ka.

3.2. Sub-regional changes

The major trends, abrupt changes, and multi-century events affected all of our sub-regions in different ways (Fig. 6). In all of the sub-regions, temperature trends after 8 ka correlated significantly but negatively with the moisture trends ($r = -0.58$ to -0.89). As mean regional temperatures declined, effective moisture rose (Fig. 6). For example, correlations and Granger tests indicate that temperature changes at Steel Lake, Minnesota (Fig. 6B, thin black line) usefully predict the effective moisture trends inferred from dust changes there (Fig. 6B, middle row): $r = -0.52$; $F = 9.26$, $p = 0.0027$.

The independent datasets consistently reconstructed multiple multi-century events (e.g., a mid-continental cold period at ca. 5.5–4.8 ka, Fig. 7), but the sequence of multi-century events and step changes observed in the mean regional record (Fig. 2) does not represent a widely or consistently expressed signal at sub-regional scales (Fig. 6). Rather, the events and steps in the mean record (Fig. 2) often represent positive interference among sub-regional patterns with different, but overlapping, periods of anomalous conditions. For example, cool events (>0.4 °C and >200 yrs) interrupted the warming before 8.0 ka at different times in different regions: a) in the west from 9.7 to 8.5 ka; b) at Steel Lake and other west-central sites at 8.6–8.1 and 8.0–7.5 ka respectively; c) in Ontario at 9.3–8.9 ka; and d) in SSTs at 9.5–9.1 ka (Fig. 6). Some of these events overlap in time and may only differ due to age uncertainties, but others are potentially out of phase with each other (e.g., Fig. 6B). Despite the differences, the data widely record a subsequent step change at 8.2–8.0 ka that produced near stationary maximum temperatures until at least 6.8 ka in central and eastern areas (Fig. 6B–D).

In the eastern coastal region, the MTWM reconstruction correlates ($r = 0.77$) with the detrended SST record (Fig. 6D). Both indicate warming of 1–2 °C with important, but different, multi-century fluctuations before 7 ka. By contrast, the raw SST reconstructions, which retain a large linear trend (Sachs, 2007), indicate that the early Holocene and Younger Dryas (YD) chronozone (12.7–11.7 ka) were >5 °C warmer than today, which is inconsistent with the magnitudes of the various isotopic changes and with the pollen-inferred temperatures from all of the sub-

Table 2
Principal Component (PCA) loadings. Sites are sorted by loadings of the variable-specific PCAs.

Component:			All		Temperature		Moisture		Isotopes	
			1	2	1	2	1	2	1	2
Percent of Variance:			34.92	21.07	35.23	28.54	51.10	19.34	42.30	23.63
Buckbean Fen/Sherd Lake	WY	T	**0.25**	−0.07	**0.61**	**−0.23**				
GGC30 (Nova Scotia)		SST	**0.24**	0.01	**0.39**	−0.04				
Mansell Pond	ME	T	**0.22**	0.01	**0.26**	0.04				
Steel Lake	MN	T	0.06	**0.32**	**0.22**	**0.70**				
Nutt Lake	ON	T	**0.23**	−0.03	0.19	−0.04				
Blood Pond	MA	T	0.10	0.17	0.15	**0.25**				
High Lake	ON	T	0.16	0.19	0.12	0.12				
Little Pond	MA	T	0.14	−0.14	0.12	−0.07				
Graham Lake	ON	T	0.13	0.17	0.11	0.10				
Sutherland Pond	NY	T	0.19	0.13	0.11	0.06				
Devils Lake	WI	T	0.15	**0.21**	0.09	0.09				
Moon Lake	ND	T	0.16	0.02	0.08	0.02				
GGC19 (Virginia)		SST	0.05	**0.26**	0.06	**0.25**				
Spruce Pond	NY	T	0.07	**0.30**	0.06	**0.20**				
Sharkey Lake	MN	T	0.07	**0.25**	0.04	0.18				
Rice Lake	ND	T	0.05	0.03	0.03	0.01				
Hams Lake	ON	T	−0.03	0.16	−0.01	0.17				
Deep Pond	MA	T	−0.06	**0.20**	−0.07	**0.21**				
Pickerel Lake	SD	T	**−0.20**	0.05	−0.18	0.05				
Lake West Okoboji	IA	T	−0.10	−0.05	**−0.20**	−0.19				
Chatsworth Bog	IL	T	−0.16	0.12	**−0.38**	**0.31**				
Upper Big Creek Lake	CO	LL	−0.05	0.13			−0.03	0.10		
Little Windy Hill Pond	WY	LL	0.09	0.14			0.18	**0.24**		
Lower Paintrock Lake	WY	LL	0.04	**−0.22**			0.19	**−0.46**		
Steel Lake	MN	D	**0.23**	0.15			**0.23**	**0.50**		
Elk Lake	MN	D	**0.22**	0.10			**0.28**	**0.39**		
New Long Pond	MA	LL	0.10	**−0.30**			**0.30**	−0.40		
Lake of the Woods	WY	LL	**0.21**	0.03			**0.31**	0.18		
Davis Pond	MA	LL	0.19	**−0.23**			**0.38**	−0.23		
Rainbow Lake	WY	LL	**0.25**	−0.05			**0.38**	0.16		
Deep Pond	MA	LL	**0.20**	**−0.23**			**0.39**	−0.21		
Emerald Lake	CO	LL	**0.25**	−0.13			**0.42**	−0.01		
Bear Lake	ID/UT	18O	−0.16	0.08					**−0.42**	**0.32**
Berry Pond	MA	2H	0.05	0.07					0.12	**0.80**
O'Brien Lake	MI	18O	**0.20**	0.19					**0.40**	**0.47**
Grinnell Lake	NJ	18O	0.19	−0.05					**0.56**	−0.19
Crawford Pond	ON	18O	**0.22**	−0.17					**0.57**	−0.07

The absolute value of loadings listed in bold exceeds 0.2.

regions (top, Fig. 6). In fact, the southern tier of west-central sites from Pickerel Lake, SD to Chatsworth Bog, IL, were at least as cool as today until after 4.8 ka even though Steel Lake, MN to the north warmed to higher than modern temperatures after 8.2 ka (Fig. 6B). PC1 loadings indicate opposing directions of temperature change (cooling versus warming since 7 ka) in northern (e.g., Mansell Pond, Maine; Scotian margin SSTs) and southern reconstructions (e.g., Chatsworth Bog, Illinois) as well as a geographically crosscutting zone with small trends (loadings <0.1) from North Dakota and southern Minnesota to Wisconsin and southern Ontario (Table 2).

The directions of some major moisture changes also differed between western and eastern areas (Fig. 6). Lake levels from inland (Fig. 6C) and coastal Massachusetts (Fig. 6D) increased by >1 sd before 9.0 and 8.2 ka respectively, but moisture levels in the west rose to an early Holocene maximum by 10 ka and then rapidly declined to their lowest levels of the past 10 ka at 9.3 ka (Fig. 6A). Effective moisture also declined after an early Holocene maximum (>9.3 ka) in the west-central region based on short-lived peaks and attendant stepwise increases in dust deposition at 9.3 and 8.2 ka at Elk and Steel Lakes, MN (Fig. 6B, note inverted scale). The dust records only extend to <11 ka, but their mean correlates with the mean lake-level record from Wyoming over the common period of record ($r = -0.57$; Fig. 6B–C); Granger tests show that the mean dust record contributes significantly to predicting the Wyoming lake changes ($F = 5.25$, $p = 0.023$). Taken together the various records show that the east-west moisture gradient had been weaker than today before ca. 9 ka because effective moisture was low in the east and high in the west. The gradient then steepened as the west dried relative to the east by ca. 8 ka.

3.2.1. Mid-Holocene events

In the west (Fig. 6A) and coastal east (Fig. 6D), stepwise cooling of >0.4 °C at 5.7–5.0 ka marked a permanent end to the period with maximum temperatures, which had ended in Ontario at 7.0–6.8 ka (Fig. 6C). Likewise, oxygen and hydrogen isotope values from Steel Lake, O'Brien Lake, Crawford Pond, Fayetteville Green Lake, and Berry Pond (Henne and Hu, 2010; Kirby et al., 2002; Nelson and Hu, 2008; Shuman et al., 2006; Yu et al., 1997) show rapid stepwise declines in delta values at ca. 5.5 ka (Fig. 4C). Because the changes are equivalent to a >0.5‰ change in $\delta^{18}O$, the shift would be consistent with cooling of >0.35 °C based on the Dansgaard (1964) temperature-$\delta^{18}O$ relationship although numerous other factors almost certainly also influenced the isotope ratios. The shifts are synchronous within the current age uncertainties of each record (following Parnell et al., 2008).

In the central region, the change at 5.5 ka initiated a prominent millennial-scale fluctuation in temperature and moisture (Fig. 7). A reduction in dust accumulation, and by inference an increase in effective moisture, at Elk and Steel Lakes, Minnesota, from 5.6 to 4.8 ka coincided with a reduction in pollen-inferred temperatures

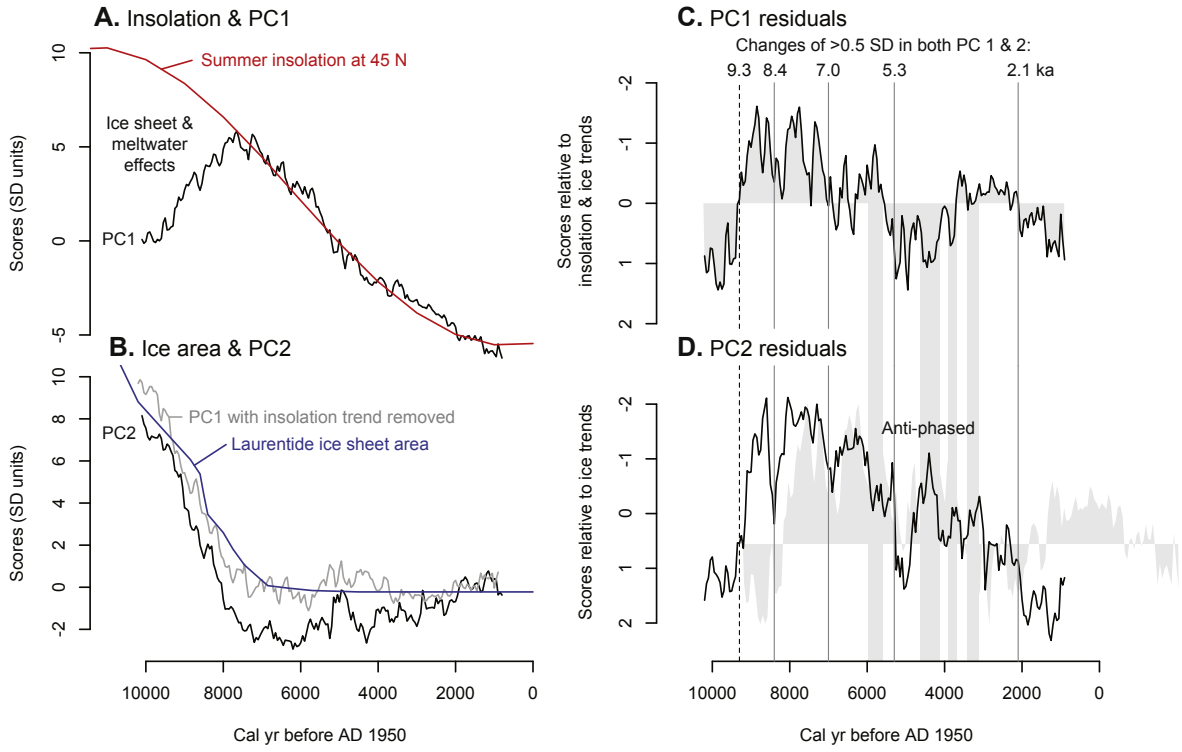

Fig. 5. PC scores plotted by time based on the complete dataset. A) Scores for the first component (PC1) are shown with the June insolation trend for 45°N (Berger and Loutre, 1991) in red. B) Scores for the second component (PC2) as well as the residuals of PC1 minus the June insolation trend (gray line) are shown with the area of the Laurentide ice sheet (Dyke, 2004) in blue. C-D) Residual scores for PC1 (top) and PC2 (bottom) after both insolation (PC1 only) and ice area trends (PC1 & 2) have been removed.

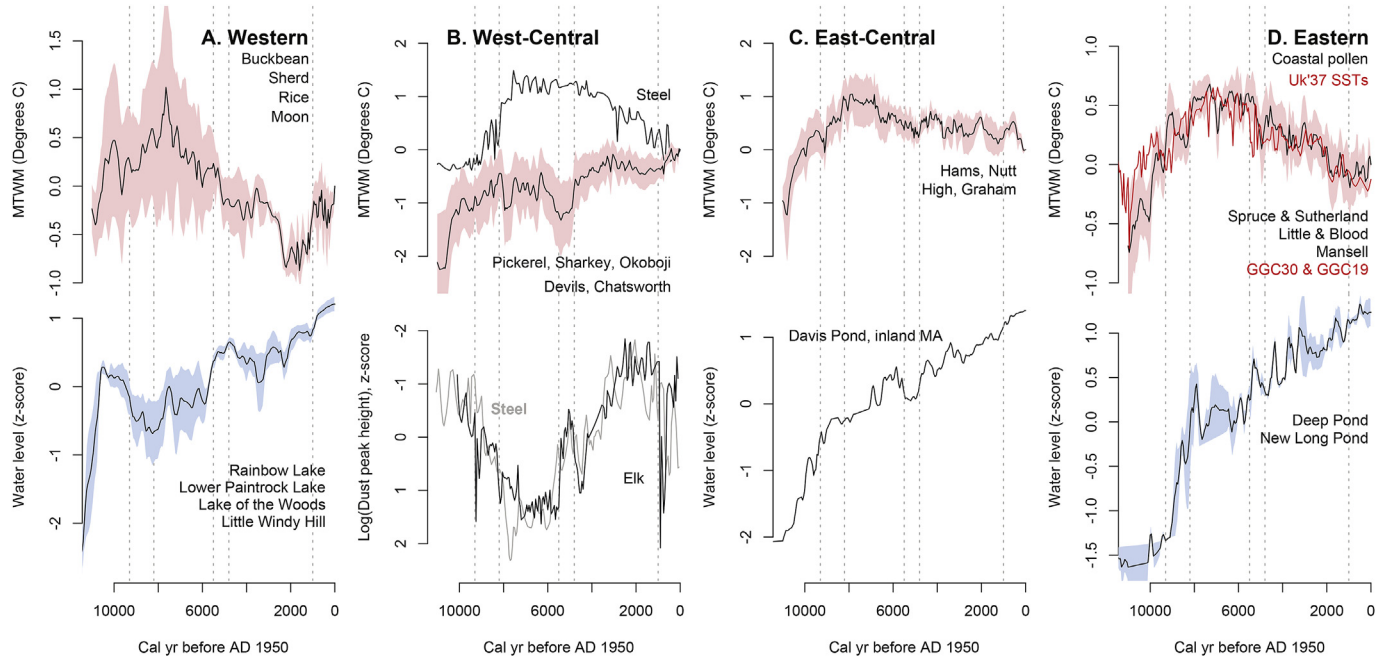

Fig. 6. Stacks of temperature (top) and moisture (bottom) records from the A) western, B) west-central, C) east-central, and D) eastern sub-regions. All temperature records are shown as deviations in degrees C from their most recent value; all moisture records are shown as z-scores (anomalies in standard deviations from their mean). Shading indicates the standard error about the mean for all stacks (except, for simplicity, SSTs shown in red in D); time series from individual sites are shown without uncertainty. Sites included in each stack are listed. MTWM indicates mean temperature of the warmest month; SST indicates detrended sea-surface temperatures. (For interpretation of the references to colour in this figure legend, the reader is referred to the web version of this article.)

in the same region (Fig. 6B), particularly at Sharkey Lake, Lake West Okoboji, and Chatsworth Bog (Fig. 7). Varve counts from Elk Lake indicate that the changes there could have taken place within centuries or less at 5.49–5.39 and 4.81–4.54 varve ka.

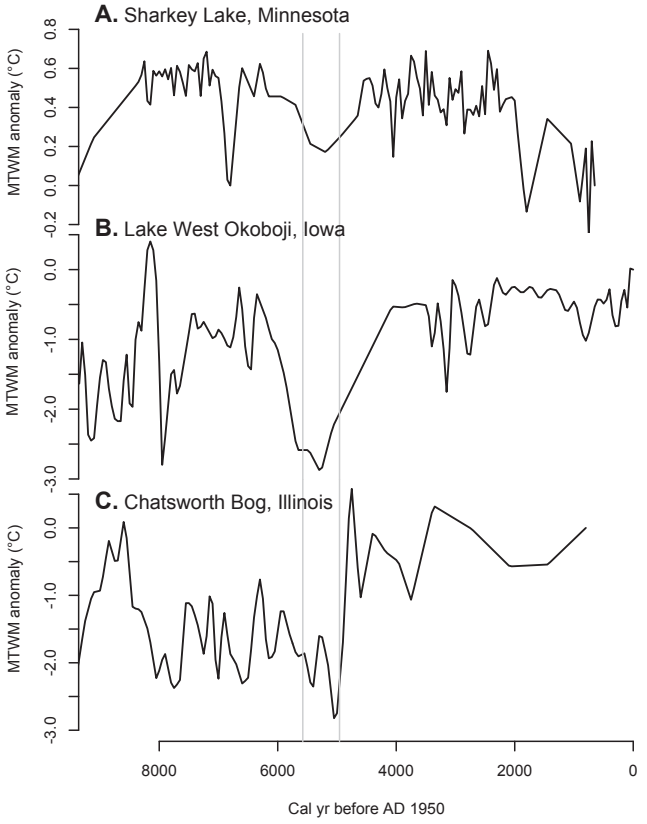

Fig. 7. Pollen-inferred mean temperatures of the warmest month (as anomalies relative to present) for three sites from the west-central sub-region.

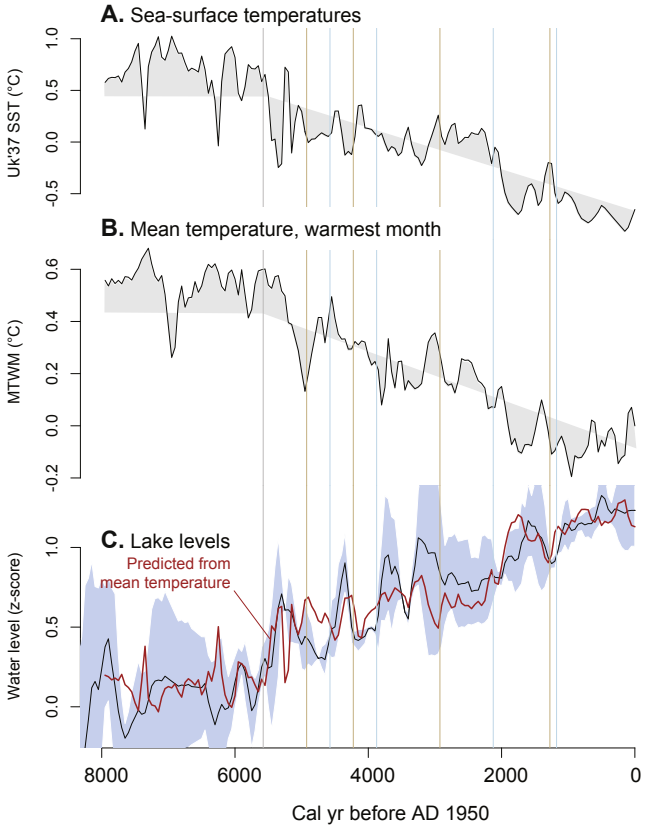

Fig. 8. Trends and multi-century climate variability in the eastern sub-region over the past 8000 years. Time series (which are the same as shown in Fig. 6D) represent the means of the available reconstructions of A) sea-surface temperatures (SST), B) mean temperature of the warmest month (MTWM), and C) lake level. The red line in C represents the linear model of the mean lake-level changes based on the mean of the temperature records (both SSTs and MTWM); for comparison, blue shading shows the standard error about the mean lake-level reconstruction. Gray shading indicates multi-century deviations from the long-term temperature trends. Vertical lines indicate the beginning (tan) and end (blue) of multi-century droughts reconstructed in coastal Massachusetts, based on the mode of the age distributions calculated for regional drought events by Newby et al. (2014). (For interpretation of the references to colour in this figure legend, the reader is referred to the web version of this article.)

The event from 5.6 to 4.8 ka also included hydroclimatic changes in the other sub-regions (Fig. 6). In the Rocky Mountain west, a narrowing of the uncertainty around the mean lake-level series indicates a coherent increase in moisture levels by >0.8 sd from 5.8 to 5.1 ka (Fig. 6A). Of all of the moisture records examined here, only Davis Pond from the inland highlands of western Massachusetts did not rise at this time (Fig. 6C), but it experienced a phase of anomalously low water constrained by similar bracketing ages: 5.7–4.9 ka (Fig. 6C).

3.2.2. Late Holocene

Changes after 5.7 ka marked the beginning of cooling and moistening trends in many areas, which persisted until present and were punctuated by a series of multi-century events (Fig. 6). In the coastal east, multi-century moisture variations of the last >5.7 ka coincided with terrestrial and marine temperature changes (Fig. 8). Warm/dry and cool/moist deviations from the long-term trends appear to represent the dominant modes of variability. The warm, dry phases became progressively cooler and wetter toward present, such that the most recent warm, dry periods (e.g., 1.3–1.2 ka) had absolute temperatures and moisture levels equal to the earliest of the intervening cool, wet phases (e.g., 4.6–4.2 ka).

The SST and MTWM records skillfully predict the moisture trends based on a linear model of the mean lake level changes (red line, Fig. 8; $p < 2.2 * 10^{-16}$, adjusted $R^2 = 0.84$). Granger tests spanning the period since 8 ka also show that mean SSTs and MTWM predict each other more than the autocorrelation in each series alone (SST as a predictor of MTWM: $F = 16.16$, $p = 0.00009$; MTWM as a predictor of SST: $F = 10.88$, $p = 0.00004$). The temperatures have a similar relationship to the lake level changes (e.g., MTWM as a predictor of lake level: $F = 5.2$, $p = 0.024$; lake level as a predictor of MTWM: $F = 7.97$, $p = 0.0054$). Consequently, the three different data types from nine different sites in the eastern sub-region contain a well-replicated signal of drought and warming at 4.9–4.6, 4.2–3.9, 2.9–2.1, and 1.3–1.2 ka.

Sharp cooling at 2.1–1.8 ka of 0.25–0.5 °C coincided with a rapid rise in water levels (>0.25 sd), and produced the dominant climate of the Common Era (0–1950 AD). SSTs and MTWMs during the preceding 800 years (the "2.7-ka event" from 2.9 to 2.1 ka) as well as during a pair of cool, moist periods in the millennium from 3.9 to 2.9 ka were 0.2–0.4 °C higher than during even the warmest portion of the Common Era (1.5–1.2 ka). Consequently, the Common Era represents the coolest and wettest portion of the last 9.3 ka in the coastal east (Fig. 8) and likely, in much of the study region except possibly in central areas such as Minnesota, Iowa, and Illinois (Fig. 6B).

4. Discussion

4.1. Coherency of the records

Signals in our dataset confirm that the Holocene climate history of mid-latitude North America included a combination of coherent

long-term trends (Fig. 5A–B); regime shifts at ca. 9.3, 8.0, 7.0, 5.3, and 2.1 ka (Fig. 5B–D); and multi-century events, such as at 8.3–8.0, 5.2–4.9, and 1.3–0.8 ka (Fig. 5C–D). Many of the trends, steps, and events affected both temperature and effective moisture patterns (Figs. 2, 6 and 8), and despite some differences among records, were recorded repeatedly and independently by sediment stratigraphies, geochemical changes, and biotic assemblage changes. The shared signals validate the robustness of many of the multi-millennial to multi-centennial features of the records.

Multi-century variability composes an important part of the spectrum of mid-latitude climate changes (Fig. 8), but some events described in other studies, such as at ca. 4.2 and 2.7 ka (Booth et al., 2005; Martin-Puertas et al., 2012; van Geel et al., 2000; Walker et al., 2012), do not consistently appear as prominent features in our study region (Figs. 2, 4 and 6). They may have been a) more important in other parts of the world than mid-latitude North America, b) composed of complex multivariate signals, or c) narrower in spatial extent than the largest events and abrupt changes detected by our rates of change and principal component analyses (Figs. 3–5). Changes and events, such as at 5.6–4.8 ka, stand out more prominently than these events in our sub-regions (e.g., Fig. 6), just as other well-studied events, such as at ca. 8.2 ka (Alley et al., 1997) and 9.3 ka (Fleitmann et al., 2008), appear to have different characteristics here than elsewhere (e.g., manifesting as more consistently as step changes rather than events).

Common signals exist at low frequencies, in part, because all of the records act as low-pass filters on the climate history via factors such as tree longevity, watershed-scale hydrologic response times, and sediment mixing. None of the archives used here, however, have a substantially greater lag or bias towards low frequency components than the others (e.g., alkenone-, pollen-, and sediment-derived datasets in Fig. 8). Indeed, the comparability of the records reveals that even small climate changes, such as temperature changes of ~0.2 °C, produced meaningful ecological changes that affected both terrestrial vegetation and marine plankton (Fig. 8A–B), while also altering the sediment and geochemical dynamics in small lakes and ponds (Fig. 8C).

The comparability of multiple records from within individual sub-regions (e.g., Figs. 7–8) indicates that additional differences among sub-regions (Fig. 6) and variables (Figs. 3–4) likely represent underlying climatic heterogeneity and structure much like that existing during modern droughts or other variations. The records examined here differ most often, and contain poorly replicated features, at centennial and shorter scales where radiocarbon uncertainties, sample spacing, and reconstruction error may all be factors. However, by averaging across multiple records in each sub-region, we have reduced the random sources of error and the remaining disparities will require more detailed analyses to diagnose.

4.2. Uncertainties and sources of error

Some important differences among records probably arose from non-climatic factors. For example, raw (not detrended) alkenone-based SST reconstructions indicate, and may faithfully capture, a substantial background cooling trend of >5 °C in the western Atlantic during the Holocene (Sachs, 2007), but our MTWM reconstructions only correlate well with the SST records once the SSTs have been linearly detrended (Fig. 6D). Both the MTWM and SST reconstructions indicate maximum warmth relative to any background trend from ca. 8–5 ka, which is consistent with macrofossil evidence that tree species in the northeastern U.S. grew at higher elevations than today at the time (Jackson and Whitehead, 1991; Shuman et al., 2004; Spear et al., 1994). By contrast, greater than modern temperatures in the raw SST records during the YD, just prior to the start of a large magnitude Holocene cooling trend (Sachs, 2007), differ from terrestrial inferences about the YD drawn from pollen, chironomid, lake productivity, and stable isotope data from the Atlantic coast of North America (Hou et al., 2007; Levesque et al., 1997; Peteet et al., 1990). Other paleoceanographic records also do not confirm the magnitude of the subsequent Holocene cooling (Kim et al., 2007, 2004; Solignac et al., 2004; Thornalley et al., 2009). Consequently, a linear or similar trend in the raw SST reconstructions may have been generated by nutrients or other factors (Prahl et al., 2006) or may represent a temperature trend unique to the region of the Labrador Current (Sachs, 2007). Only the superimposed variability correlates with other regional records (Figs. 6D and 8). If the detrended SST signal (Fig. 6D) is the most climatically meaningful component of the record, then mean Holocene temperature reconstructions that incorporate the raw SST reconstructions (i.e., Marcott et al., 2013) may be artificially too high in the early Holocene (Liu et al., 2014).

The different long-term trends in the MTWM and raw SST records do not reflect a lag or similar bias in the pollen data, because such biases would have delayed, dampened, or removed the signal of the abrupt changes and multi-century events (Webb III, 1986), which we have identified as a replicated component of the dataset. The same multi-century events in the pollen-inferred data appear in the SST and lake-level reconstructions (Fig. 8); pollen-inferred precipitation changes from these sites also show a strong coherence with the lake-level reconstructions (Marsicek et al., 2013). Correlations among variables in the modern pollen analog dataset (e.g., MTWM with winter temperatures or annual precipitation; Williams and Shuman, 2008), however, may have produced other erroneous trends in our records, especially if winter temperature or effective moisture signals were erroneously translated to the summer temperature reconstructions (Telford and Birks, 2005; Williams and Shuman, 2008).

4.3. Insolation and ice sheet effects

As many studies have suggested for the past several decades, the most robust long-term features and abrupt changes in the regional record (Fig. 2) can be directly attributed to the effects of insolation and the Laurentide Ice Sheet (Fig. 5). Long-term temperature trends conform with expectations derived from climate model simulations, which show that the albedo, topography, and freshwater flux changes associated with the remnant Laurentide Ice Sheet could have kept many regions cool in the early Holocene by altering regional energy budgets and synoptic circulation patterns (Alder and Hostetler, 2015; Liu et al., 2014; Renssen et al., 2009). As a result, peak Holocene temperatures, particularly during the warmest months, were not achieved in most sub-regions until 7 ka when the thermal effects of summer insolation anomalies dominated (compare Fig. 2A with results from Liu et al., 2014).

Short-lived temperature, moisture, and isotopic events between ca. 9.5 and 8.0 ka (Figs. 4–6) may represent part of the North American expression of hemispheric cool events at ca. 9.3 and 8.2 ka (Alley et al., 1997; Fleitmann et al., 2008; Morrill et al., 2013), which were associated with glacial meltwater floods and routing changes driven by ice sheet dynamics (Barber et al., 1999; Yu et al., 2010). The events appear to be less significant and more spatially variable in North America than coincident climatic step changes (Figs. 4–6), which probably represent the consequences of rapid, non-reversing changes in ice sheet height and extent (Dyke, 2004; Shuman et al., 2002; Williams et al., 2010). Similar step changes have been documented at these times in other regions as well (Adkins et al., 2006), but their importance in North America relative to the cold events conforms with expectations that meltwater-related changes in North Atlantic circulation would have

produced events centered downwind of the North Atlantic (LeGrande and Schmidt, 2008; Wagner et al., 2013), while non-reversing changes in the height and area of the ice sheet likely produced climatic changes centered on North America (Alder and Hostetler, 2015; Felzer et al., 1996; Pausata et al., 2011).

4.4. Additional multi-century variability

The repeated multi-century warm/dry events indicated by SST-, MTWM-, and lake-level records in the east over the past 8 ka also represent a robust aspect of the Holocene record (Fig. 8), but their spatial extent and the character of similar multi-century variability in other regions requires more study. Similar variability appears in other datasets (Fig. 6), but outside of the east, few opportunities currently exist to develop a similar multi-site, multi-parameter evaluation of the signals. One exception is the cold event in the mid-continent (Fig. 7) that coincided with reduced dust deposition in Minnesota at ca. 5.6–4.8 ka (Fig. 6B).

4.5. Changes at ca. 5.5 ka

The most prominent deviations from the long-term temperature and moisture trends since 7 ka took place at 5.6–4.8 ka (Fig. 2). Stepwise transitions at ca. 5.7–5.2 ka, particularly in effective moisture, terminated extensive mid-continent aridity and the "Holocene thermal maximum" across much of our study region (Fig. 6). They, thus, widely reversed the effects produced by the decay of the ice sheet and its meltwater before ca. 7 ka (Fig. 6). Some regions such as Ontario had begun to cool before 5.5 ka (Fig. 6), but even there, the largest changes in the available isotope records (Figs. 3C and 4C) likely indicate important changes in atmospheric circulation at ca. 5.5 ka (Kirby et al., 2002; Yu et al., 1997; Zhao et al., 2010). Many of the hydroclimate changes began synchronously at 5.7 ka (see synchrony analyses by Newby et al., 2014; Shuman et al., 2014).

Explanations for non-reversing shifts at 5.5 ka include amplification of orbital and greenhouse gas forcing by surface-atmosphere interactions, such as related to vegetation or sea ice changes (Claussen et al., 1999; Crucifix et al., 2002), or intrinsic ocean dynamics, such as driven by salt and heat fluxes in the North Atlantic (Goosse et al., 2002; Jongma et al., 2007; Thornalley et al., 2009). Such mechanisms have been proposed and debated as an explanation for the end of the African Humid Period at ca. 5.5 ka (deMenocal et al., 2000; Kropelin et al., 2008; McGee et al., 2013; Shanahan et al., 2015; Tierney and deMenocal, 2013), but changes at this time extended across the Northern Hemisphere (Magny and Haas, 2004; Magny et al., 2006; Oppo et al., 2003; Shuman, 2012b; Thornalley et al., 2009). Our results confirm their importance for mid-latitude North America.

4.6. Climates of the Common Era

The past 2000 years (the 'Common Era') represent the period with the highest average effective moisture and coolest summers since the decay of the ice sheet (Fig. 2). The rates of cooling and moistening accelerated by ca. 2.1 ka, and the changes have many similarities to those at ca. 5.5 ka (Figs. 2 and 5). Consequently, the conditions of the Common Era were not representative of conditions that had persisted for much of the Holocene, and medieval warmth and drought that punctuated the conditions of the Common Era, especially in portions of the east (Fig. 8), rarely reached the magnitude of earlier events (Figs. 6 and 8).

The climate changes of the Common Era differed, however, across sub-regions (Fig. 6), and thus further confirm the importance of spatial patterning of Holocene climate variations at centennial to millennial scales. Temperatures from Wyoming to Illinois, like dust accumulation rates in Minnesota, were lower before 1 ka than afterward (Fig. 6A,B). Elsewhere, the lowest temperatures and highest effective moisture levels were achieved after 1 ka and then again after the multi-century phase of high temperatures and drought during medieval times, which appears most prominently in MTWM, SST, and lake-level records from the east (Fig. 8). Although the medieval anomaly appears to have been earlier in the coastal east than elsewhere (Fig. 6A–C), the duration of the event is also short relative to the associated temporal uncertainty and the age differences cannot be verified.

5. Conclusions

The consistent climate signals detected across regions and diverse (sedimentary, geochemical, biotic) paleoenvironmental records (Figs. 2–5) indicate an integrated sequence of slow trends, abrupt shifts and accelerations, and multi-century events during the Holocene climate history of mid-latitude North America. The sequence of events captured by our mean temperature and moisture records (Figs. 2 and 6), rate-of-change analyses (Fig. 3), and principal component analyses (Figs. 4–5) confirms that a series of abrupt shifts and transient fluctuations produced important modifications of orbital and ice sheet driven climate trends from the Rocky Mountains to the North Atlantic. However, the same details do not apply to all locations or records (Fig. 6), and >30% of the variance in the data derives from local to sub-regional patterns (Table 2).

Within the context of sub-regional variation (Fig. 6), widespread, multi-parameter replication of the structure of the climate history indicates that abrupt events had magnitudes equal to about 25–50% of the long-term changes. They included both positive and negative interference with the long trends, and despite their modest magnitudes, must have produced significant ecological (vegetation/pollen) and geomorphic (lake/dust) consequences to enable detection by the records examined here. Rapid transitions from ca. 9.3–8.2 ka coincided with the declining influence of the Laurentide Ice Sheet and its meltwater, but additional step changes and acceleration of long-term trends at ca. 5.5 and 2.1 ka were equally as important and may have resulted from far-field feedbacks related to Northern Hemisphere cooling. The replicated evidence for multi-century, multivariate climate changes provides a benchmark for comparison with simulations aimed at understanding the full spectrum of climate variations, but more detailed data are required to fully map and understand the structure of these spatially varied changes.

Acknowledgements

This project was supported by NSF (BCS-0845129; DEB-1146297) and Wyoming Water Research Program/USGS funding to B.S., as well as a NASA Space Grant Fellowship to J.M. (#NNX10AO95H). We thank contributors of data to the NOAA Paleoclimate and Neotoma Databases; P. Henne, M. Serravezza and W. Oswald for making data available; two anonymous reviewers, D. R. Foster, and T. Webb III for comments on the manuscript.

References

Adkins, J., deMenocal, P., Eshel, G., 2006. The African humid period and the record of marine upwelling from excess ^{230}Th in Ocean Drilling Program Hole 658C. Paleoceanography 21, PA4203. http://dx.doi.org/10.1029/2005pa001200.

Alder, J.R., Hostetler, S.W., 2015. Global climate simulations at 3000-year intervals for the last 21 000 years with the GENMOM coupled atmosphere–ocean model. Clim. Past Discuss. 11, 449–471.

Alley, R.B., 2003. Raising paleoceanography. Paleoceanography 18, 1085. http://

dx.doi.org/10.1029/2003pa000942.
Alley, R.B., Mayewski, P.A., Sowers, T., Stuiver, M., Taylor, K.C., Clark, P.U., 1997. Holocene climatic instability: a prominent, widespread event 8200 yr ago. Geology 25, 483–486. http://dx.doi.org/10.1130/0091-7613(1997)025<0483:hciapw>2.3.co;2.
Almquist-Jacobson, H., Sanger, D., 1995. Holocene climate and vegetation in the Milford drainage basin, Maine, USA, and their implications for human history. Veg. Hist. Archaeobot. 4, 211–222.
Anderson, L., 2012. Rocky mountain hydroclimate: Holocene variability and the role of insolation, ENSO, and the North American Monsoon. Glob. Planet. Change 92–93, 198–208. http://dx.doi.org/10.1016/j.gloplacha.2012.05.012.
Anderson, L., 2011. Holocene record of precipitation seasonality from lake calcite $\delta^{18}O$ in the central Rocky Mountains, United States. Geology 39, 211–214. http://dx.doi.org/10.1130/g31575.1.
Baker, R.G., 1976. Late Quaternary Vegetation History of the Yellowstone Lake Basin, Wyoming. United States Geological Survey Professional Paper 729-E.
Baker, R.G., Maher Jr., L.J., Chumbley, C.A., Van Zant, K.L., 1992. Patterns of Holocene environmental change in the Midwestern United States. Quat. Res. 37, 379–389.
Barber, D.C., Dyke, A., Hillaire-Marcel, C., Jennings, A.E., Andrews, J.T., Kerwin, M.W., Bilodeau, G., McNeely, R., Southon, J., Morehead, M.D., Gagnon, J.M., 1999. Forcing of the cold event of 8,200 years ago by catastrophic drainage of Laurentide lakes. Nature 400, 344–348.
Bartlein, P., Harrison, S., Brewer, S., Connor, S., Davis, B., Gajewski, K., Guiot, J., Harrison-Prentice, T., Henderson, A., Peyron, O., Prentice, I., Scholze, M., Seppa, H., Shuman, B., Sugita, S., Thompson, R., Viau, A., Williams, J., Wu, H., 2011. Pollen-based continental climate reconstructions at 6 and 21 ka: a global synthesis. Clim. Dyn. 37, 775–802. http://dx.doi.org/10.1007/s00382-010-0904-1.
Bennett, K.D., 1983. Competitive interactions among forest tree populations in Norfolk, England, during the last 10,000 Years. New Phytol. 103, 603–620.
Berger, A., Loutre, M.F., 1991. Insolation values for the climate of the last 10 million years. Quat. Sci. Rev. 10, 297.
Booth, R.K., Jackson, S.T., Forman, S.L., Kutzbach, J.E., Bettis, E.A., Kreig, J., Wright, D.K., 2005. A severe centennial-scale drought in midcontinental North America 4200 years ago and apparent global linkages. Holocene 15, 321.
Booth, R.K., Notaro, M., Jackson, S.T., Kutzbach, J.E., 2006. Widespread drought episodes in the western great lakes region during the past 2000 year: geological extent and potential mechanisms. Earth Planet. Sci. Lett. 242, 415–427.
Bright, J., Kaufman, D.S., Forester, R.M., Dean, W.E., 2006. A continuous 250,000-yr record of oxygen and carbon isotopes in ostracode and bulk-sediment carbonate from Bear Lake, Utah-Idaho. Quat. Sci. Rev. 25, 2258–2270. http://dx.doi.org/10.1016/j.quascirev.2005.12.011.
Bryson, R.A., 1966. Air masses, streamlines, and the boreal forest. Geol. Soc. Am. Bull. 8, 228.
Burkart, M.R., 1976. Pollen Biostratigraphy and Late Quaternary Vegetation History of the Bighorn Mountains, Wyoming. University of Iowa, Geology, Iowa City, Iowa, USA.
Camill, P., Umbanhowar Jr., C.E., Teed, R., Geiss, C.E., Aldinger, J., Dvorak, L., Kenning, J., Limmer, J., Walkup, K., 2003. Late-glacial and Holocene climatic effects on fire and vegetation dynamics at the prairie-forest ecotone in south-central Minnesota. J. Ecol. 91, 822–836.
Claussen, M., Kubatzki, C., Brovkin, V., Ganopolski, A., Hoelzmann, P., Pachur, H.J., 1999. Simulation of an abrupt change in Saharan vegetation in the mid-Holocene. Geophys. Res. Lett. 26, 2037–2040.
COHMAP, M., 1988. Climate changes of the last 18,000 years: observations and model simulations. Science 241, 1043–1052.
Cook, E.R., Krusic, P.J., 2004. The North American Drought Atlas [WWW Document].
Crucifix, Loutre, Tulkens, Fichefet, Berger, 2002. Climate evolution during the Holocene: a study with an Earth system model of intermediate complexity. Clim. Dyn. 19, 43–60. http://dx.doi.org/10.1007/s00382-001-0208-6.
Dansgaard, W., 1964. Stable isotopes in precipitation. Tellus 16, 436–468. http://dx.doi.org/10.1111/j.2153-3490.1964.tb00181.x.
Dean, W.E., 1997. Rates, timing, and cyclicity of Holocene eolian activity in north-central United States; evidence from varved lake sediments. Geology 25, 331–334.
deMenocal, P., Ortiz, J., Guilderson, T., Adkins, J., Sarnthein, M., Baker, L., Yarusinsky, M., 2000. Abrupt onset and termination of the African Humid Period:: rapid climate responses to gradual insolation forcing. Quat. Sci. Rev. 19, 347–361.
Digerfeldt, G., 1986. Studies on past lake-level fluctuations. In: Berglund, B.E. (Ed.), Handbook of Holocene Palaeoecology and Palaeohydrology. John Wiley and Sons, Chichester, U. K., pp. 127–142
Donders, T.H., Wagner-Cremer, F., Visscher, H., 2008. Integration of proxy data and model scenarios for the mid-Holocene onset of modern ENSO variability. Quat. Sci. Rev. 27, 571–579.
Dyke, A.S., 2004. An outline of North American deglaciation with emphasis on central and northern Canada. In: Ehlers, J., Gibbard, P.L. (Eds.), Developments in Quaternary Science. Elsevier, pp. 373–424.
Felzer, B., Oglesby, R.J., Webb, T., Hyman, D.E., 1996. Sensitivity of a general circulation model to changes in northern hemisphere ice sheets. J. Geophys. Res. 101, 19077–19092. http://dx.doi.org/10.1029/96JD01219.
Fleitmann, D., Mudelsee, M., Burns, S.J., Bradley, R.S., Kramers, J., Matter, A., 2008. Evidence for a widespread climatic anomaly at around 9.2 ka before present. Paleoceanography 23, PA1102. http://dx.doi.org/10.1029/2007pa001519.
Forman, S.L., Oglesby, R., Webb, R.S., 2001. Temporal and spatial patterns of Holocene dune activity on the Great Plains of North America: megadroughts and climate links. Glob. Planet. Change 29, 1–29.
Foster, D.R., Oswald, W.W., Faison, E.K., Doughty, E.D., Hansen, B.C.S., 2006. A climatic driver for abrupt mid-Holocene vegetation dynamics and the hemlock decline in New England. Ecology 87, 2959–2966.
Fuller, J.L., 1998. Ecological impact of the mid-Holocene hemlock decline in southern Ontario, Canada. Ecology 79, 2337–2351. http://dx.doi.org/10.1890/0012-9658(1998)079[2337:EIOTMH]2.0.CO;2.
Gibson, J.J., Edwards, T.W.D., 2002. Regional water balance trends and evaporation-transpiration partitioning from a stable isotope survey of lakes in northern Canada. Glob. Biogeochem. Cycles 16, 1026. http://dx.doi.org/10.1029/2001gb001839.
Gibson, J.J., Prepas, E.E., McEachern, P., 2002. Quantitative comparison of lake throughflow, residency, and catchment runoff using stable isotopes: modelling and results from a regional survey of Boreal lakes. J. Hydrol. 262, 128–144.
Goosse, H., Renssen, H., Selten, F.M., Haarsma, R.J., Opsteegh, J.D., 2002. Potential causes of abrupt climate events: a numerical study with a three-dimensional climate model. Geophys. Res. Lett. 29, 1860. http://dx.doi.org/10.1029/2002gl014993.
Granger, C., 1969. Investigating causal relations by econometric models and cross-spectral methods. Econometrica 37, 424–438.
Grimm, E.C., 2001. Trends and palaeoecological problems in the vegetation and climate history of the northern Great Plains, U.S.A. Biol. Environ. Proc. R. Ir. Acad. 99B, 1–18.
Grimm, E.C., Maher Jr., L.J., Nelson, D.M., 2009. The magnitude of error in conventional bulk-sediment radiocarbon dates from central North America. Quat. Res. 72, 301–308.
Grimm, E.C., Donovan, J.J., Brown, K.J., 2011. A high-resolution record of climate variability and landscape response from Kettle Lake, northern Great Plains, North America. Quat. Sci. Rev. 30, 2626–2650.
Halfen, A.F., Johnson, W.C., 2013. A review of Great Plains dune field chronologies. Aeolian Res. 10, 135–160. http://dx.doi.org/10.1016/j.aeolia.2013.03.001.
Haslett, J., Parnell, A., 2008. A simple monotone process with application to radiocarbon-dated depth chronologies. J. R. Stat. Soc. Ser. C Appl. Stat. 57, 399–418. http://dx.doi.org/10.1111/j.1467-9876.2008.00623.x.
Henderson, A.K., Shuman, B., 2009. Hydrogen and oxygen isotopic compositions of lake water in the western United States. Bull. Geol. Soc. Am. 121, 1179–1189.
Henne, P.D., Hu, F.S., 2010. Holocene climatic change and the development of the lake-effect Snowbelt in Michigan, USA. Quat. Sci. Rev. 29, 940–951. http://dx.doi.org/10.1016/j.quascirev.2009.12.014.
Hou, J., Huang, Y., Oswald, W.W., Foster, D.R., Shuman, B., 2007. Centennial-scale compound-specific hydrogen isotope record of Pleistocene-Holocene climate transition from southern New England. Geophys. Res. Lett. 34, L19706. http://dx.doi.org/10.1029/2007GL030303.
Jackson, S.T., Whitehead, D.R., 1991. Holocene vegetation patterns in the Adirondack Mountains. Ecology 72, 641–653.
Jasechko, S., Sharp, Z.D., Gibson, J.J., Birks, S.J., Yi, Y., Fawcett, P.J., 2013. Terrestrial water fluxes dominated by transpiration. Nature 496, 347–350. http://dx.doi.org/10.1038/nature11983.
Jongma, J.I., Prange, M., Renssen, H., Schulz, M., 2007. Amplification of Holocene multicentennial climate forcing by mode transitions in North Atlantic overturning circulation. Geophys. Res. Lett. 34, L15706. http://dx.doi.org/10.1029/2007gl030642.
Kaufman, D.S., Ager, T.A., Anderson, N.J., Anderson, P.M., Andrews, J.T., Bartlein, P.J., Brubaker, L.B., Coats, L.L., Cwynar, L.C., Duvall, M.L., Dyke, A.S., Edwards, M.E., Eisner, W.R., Gajewski, K., Geirsdóttir, A., Hu, F.S., Jennings, A.E., Kaplan, M.R., Kerwin, M.W., Lozhkin, A.V., MacDonald, G.M., Miller, G.H., Mock, C.J., Oswald, W.W., Otto-Bliesner, B.L., Porinchu, D.F., Rühland, K., Smol, J.P., Steig, E.J., Wolfe, B.B., 2004. Holocene thermal maximum in the western Arctic (0–180°W). Quat. Sci. Rev. 23, 529–560. http://dx.doi.org/10.1016/j.quascirev.2003.09.007.
Kelly, R.L., Surovell, T.A., Shuman, B., Smith, G.M., 2013. A continuous climatic impact on Holocene human population in the Rocky Mountains. Proc. Natl. Acad. Sci. 110, 443–447. http://dx.doi.org/10.1073/pnas.1201341110.
Kim, J., Meggers, H., Rimbu, N., Lohmann, G., Freudenthal, T., Mueller, P.J., Schneider, R.R., 2007. Impacts of the north Atlantic gyre circulation on Holocene climate off northwest Africa. Geology 35, 387–390. http://dx.doi.org.libproxy.uwyo.edu/10.1605/01.301-0001952419.2007.
Kim, J.-H., Rimbu, N., Lorenz, S.J., Lohmann, G., Nam, S.-I., Schouten, S., Rühlemann, C., Schneider, R.R., 2004. North Pacific and North Atlantic sea-surface temperature variability during the Holocene. Quat. Sci. Rev. 23, 2141–2154.
Kirby, M.E., Mullins, H.T., Patterson, W.P., Burnett, A.W., 2002. Late glacial-Holocene atmospheric circulation and precipitation in the northeast United States inferred from modern calibrated stable oxygen and carbon isotopes. Geol. Soc. Am. Bull. 114, 1326–1340. http://dx.doi.org/10.1130/0016-7606(2002)114<1326:lghaca>2.0.co;2.
King, J.E., 1981. Late Quaternary vegetational history of Illinois. Ecol. Monogr. 51, 43–62.
Kohfeld, K.E., Harrison, S.P., 2000. How well can we simulate past climates? Evaluating the models using glabal palaeoenvironmental data sets. Quat. Sci. Rev. 19, 321–346.
Kropelin, S., Verschuren, D., Lezine, A.M., Eggermont, H., Cocquyt, C., Francus, P., Cazet, J.P., Fagot, M., Rumes, B., Russell, J.M., Darius, F., Conley, D.J., Schuster, M., von Suchodoletz, H., Engstrom, D.R., 2008. Climate-driven ecosystem

succession in the Sahara: the past 6000 years. Science 320, 765–768. http://dx.doi.org/10.1126/science.1154913.
Laird, K.R., Fritz, S.C., Grimm, E.C., Mueller, P., 1996. Century-scale paleoclimatic reconstruction from Moon Lake, a closed-basin lake in the northern Great Plains. Limnol. Oceanogr. 41, 890–902.
LeGrande, A.N., Schmidt, G.A., 2009. Sources of Holocene variability of oxygen isotopes in paleoclimate archives. Clim. Past. 5, 441–455. http://dx.doi.org/10.5194/cp-5-441-2009.
LeGrande, A.N., Schmidt, G.A., 2008. Ensemble, water isotope enabled, coupled general circulation modeling insights into the 8.2 ka event. Paleoceanography 23, PA3207. http://dx.doi.org/10.1029/2008pa001610.
Levesque, A.J., Cwynar, L.C., Walker, I.R., 1997. Exceptionally steep north-south gradients in lake temperatures during the last deglaciation. Nature 385, 423–426.
Liu, Z., Bowen, G.J., Welker, J.M., 2010. Atmospheric circulation is reflected in precipitation isotope gradients over the conterminous United States. J. Geophys. Res. Atmos. 115, D22120. http://dx.doi.org/10.1029/2010jd014175.
Liu, Z., Zhu, J., Rosenthal, Y., Zhang, X., Otto-Bliesner, B.L., Timmermann, A., Smith, R.S., Lohmann, G., Zheng, W., Timm, O.E., 2014. The Holocene temperature conundrum. PNAS 111, E3501–E3505. http://dx.doi.org/10.1073/pnas.1407229111.
Maenza-Gmelch, T.E., 1997. Holocene vegetation, climate, and fire history of the Hudson Highlands, southeastern New York, USA. The Holocene 7, 25–37.
Magny, M., Haas, J.N., 2004. A major widespread climatic change around 5300 cal. yr BP at the time of the Alpine Iceman. J. Quat. Sci. 19, 423–430. http://dx.doi.org/10.1002/jqs.850.
Magny, M., Leuzinger, U., Bortenschlager, S., Haas, J.N., 2006. Tripartite climate reversal in Central Europe 5600–5300 years ago. Quat. Res. 65, 3–19.
Mann, M.E., Zhang, Z., Rutherford, S., Bradley, R.S., Hughes, M.K., Shindell, D., Ammann, C., Faluvegi, G., Ni, F., 2009. Global signatures and dynamical origins of the little ice age and medieval climate anomaly. Science 326, 1256–1260. http://dx.doi.org/10.1126/science.1177303.
Marcott, S.A., Shakun, J.D., Clark, P.U., Mix, A.C., 2013. A reconstruction of regional and global temperature for the past 11,300 years. Science 339, 1198–1201. http://dx.doi.org/10.1126/science.1228026.
Marsicek, J.P., Shuman, B., Brewer, S., Foster, D.R., Oswald, W.W., 2013. Moisture and temperature changes associated with the mid-Holocene Tsuga decline in the northeastern United States. Quat. Sci. Rev. 80, 129–142. http://dx.doi.org/10.1016/j.quascirev.2013.09.001.
Martin-Puertas, C., Matthes, K., Brauer, A., Muscheler, R., Hansen, F., Petrick, C., Aldahan, A., Possnert, G., van Geel, B., 2012. Regional atmospheric circulation shifts induced by a grand solar minimum. Nat. Geosci. 5, 397–401. http://dx.doi.org/10.1038/ngeo1460.
Mason, J.A., Jacobs, P.M., Hanson, P.R., Miao, X.M., Goble, R.J., 2003. Sources and paleoclimatic significance of Holocene Bignell Loess, central Great Plains, USA. Quat. Res. 60, 330.
Mayewski, P.A., Rohling, E., Stager, C., Karlen, K., Maasch, K., Meeker, L.D., Meyerson, E., Gasse, F., van Kreveld, S., Holmgren, K., Lee-Thorp, J., Rosqvist, G., Rack, F., Staubwasser, M., Shneider, R., 2004. Holocene climate variability. Quat. Res. 62, 243.
McGee, D., deMenocal, P.B., Winckler, G., Stuut, J.B.W., Bradtmiller, L.I., 2013. The magnitude, timing and abruptness of changes in North African dust deposition over the last 20,000 yr. Earth Planet. Sci. Lett. 371–372, 163–176. http://dx.doi.org/10.1016/j.epsl.2013.03.054.
McKean, R.L.S., Goble, R.J., Mason, J.B., Swinehart, J.B., Loope, D.B., 2015. Temporal and spatial variability in dune reactivation across the Nebraska Sand Hills, USA. Holocene 25, 523–535. http://dx.doi.org/10.1177/0959683614561889.
Minckley, T., Shriver, R.K., Shuman, B., 2012. Resilience and regime change in a southern Rocky Mountain ecosystem during the past 17000 years. Ecol. Monogr. 82, 49–68. http://dx.doi.org/10.1890/11-0283.1.
Morrill, C., Anderson, D.M., Bauer, B.A., Buckner, R., Gille, E.P., Gross, W.S., Hartman, M., Shah, A., 2013. Proxy benchmarks for intercomparison of 8.2 ka simulations. Clim. Past. 9, 423–432. http://dx.doi.org/10.5194/cp-9-423-2013.
Mott, R.J., Grant, D.R., Stea, R., Occhietti, S., 1986. Late-glacial climatic oscillation in Atlantic Canada equivalent to the Allerod YOUNGER DRYAS EVENT. Nature 323, 247–250.
Muhs, D.R., Bettis, E.A., Aleinikoff, J.N., McGeehin, J.P., Beann, J., Skipp, G., Marshall, B.D., Roberts, H.M., Johnson, W.C., Benton, R., 2008. Origin and paleoclimatic significance of late Quaternary loess in Nebraska: evidence from stratigraphy, chronology, sedimentology, and geochemistry. Geol. Soc. Am. Bull. 120, 1378–1407. http://dx.doi.org/10.1130/B26221.1.
Munoz, S.E., Gajewski, K., Peros, M.C., 2011. Synchronous environmental and cultural change in the prehistory of the northeastern United States. Proc. Natl. Acad. Sci. 107, 22008–22201.
NCDC, 1994. Time Bias Corrected Divisional Temperature-Precipitation-Drought Index. Documentation for dataset TD-9640. DBMB, NCDC, NOAA, Federal Building, 37 Battery Park Ave. Asheville, NC 28801-2733, Asheville, NC 28801–2733.
Neff, U., Burns, S.J., Mangini, A., Mudelsee, M., Fleitmann, D., Matter, A., 2001. Strong coherence between solar variability and the monsoon in Oman between 9 and 6kyr ago. Nature 411, 290.
Nelson, D.B., Abbott, M.B., Steinman, B., Polissar, P.J., Stansell, N.D., Ortiz, J.D., Rosenmeier, M.F., Finney, B.P., Riedel, J., 2011. Drought variability in the Pacific Northwest from a 6,000-yr lake sediment record. Proc. Natl. Acad. Sci. 108, 3870–3875. http://dx.doi.org/10.1073/pnas.1009194108.
Nelson, D.M., Hu, F.S., 2008. Patterns and drivers of Holocene vegetational change near the prairie-forest ecotone in Minnesota: revisiting McAndrews' transect. New Phytol. 179, 449–459.
Newby, P.E., Donnelly, J.P., Shuman, B.N., MacDonald, D., 2009. Evidence of centennial-scale drought from southeastern Massachusetts during the Pleistocene/Holocene transition. Quat. Sci. Rev. 28, 1675–1692.
Newby, P., Shuman, B., Donnelly, J.P., Karnauskas, K.B., Marsicek, J.P., 2014. Centennial-to-Millennial hydrologic trends and variability along the north Atlantic coast, U.S.A., during the Holocene. Geophys. Res. Lett. 41 http://dx.doi.org/10.1002/2014GL060183.
Nichols, J.E., Huang, Y., 2012. Hydroclimate of the northeastern United States is highly sensitive to solar forcing. Geophys. Res. Lett. 39, L04707. http://dx.doi.org/10.1029/2011GL050720.
Oppo, D.W., McManus, J.F., Cullen, J.L., 2003. Palaeo-oceanography: deepwater variability in the Holocene epoch. Nature 422, 277.
Oswald, W.W., Faison, E.K., Foster, D.R., Doughty, E.D., Hall, B.R., Hansen, B.C.S., 2007. Post-glacial changes in spatial patterns of vegetation across southern New England. J. Biogeogr. 34, 900–913.
Overpeck, J.T., Webb III, T., Prentice, I.C., 1985. Quantitative interpretation of fossil pollen spectra: dissimilarity coefficients and the method of modern analogs. Quat. Res. 23, 87–108.
Parnell, A.C., Haslett, J., Allen, J.R.M., Buck, C.E., Huntley, B., 2008. A flexible approach to assessing synchroneity of past events using Bayesian reconstructions of sedimentation history. Quat. Sci. Rev. 27, 1872–1885. http://dx.doi.org/10.1016/j.quascirev.2008.07.009.
Pausata, F.S.R., Li, C., Wettstein, J.J., Kageyama, M., Nisancioglu, K.H., 2011. The key role of topography in altering North Atlantic atmospheric circulation during the last glacial period. Clim. Past. 7, 1089–1101. http://dx.doi.org/10.5194/cp-7-1089-2011.
Peteet, D.M., Vogel, J.S., Nelson, D.E., Southron, J.R., Nickmann, R.J., Heusser, L.E., 1990. Younger Dryas climatic reversal in northeastern USA? AMS ages for an older problem. Quat. Res. 33, 219.
Prahl, F.G., Mix, A.C., Sparrow, M.A., 2006. Alkenone paleothermometry: biological lessons from marine sediment records off western South America. Geochim. Cosmochim. Acta 70, 101–117. http://dx.doi.org/10.1016/j.gca.2005.08.023.
Pribyl, P., Shuman, B.N., 2014. A computational approach to Quaternary lake-level reconstruction applied in the central Rocky Mountains, Wyoming, USA. Quat. Res. 82, 249–259. http://dx.doi.org/10.1016/j.yqres.2014.01.012.
R Core Development Team, 2009. R: a Language and Environment for Statistical Computing. R Foundation for Statistical Computing, Vienna, Austria.
Rach, O., Brauer, A., Wilkes, H., Sachse, D., 2014. Delayed hydrological response to Greenland cooling at the onset of the Younger Dryas in western Europe. Nat. Geosci. 7, 109–112. http://dx.doi.org/10.1038/ngeo2053.
Renssen, H., Seppa, H., Heiri, O., Roche, D.M., Goosse, H., Fichefet, T., 2009. The spatial and temporal complexity of the Holocene thermal maximum. Nat. Geosci. 2, 411–414.
Sachs, J.P., 2007. Cooling of northwest Atlantic slope waters during the Holocene. Geophys. Res. Lett. 34, L03609. http://dx.doi.org/10.1029/2006gl028495.
Schlaepfer, D.R., Ewers, B.E., Shuman, B.N., Williams, D.G., Frank, J.M., Massman, W.J., Lauenroth, W.K., 2014. Terrestrial water fluxes dominated by transpiration: comment. Ecosphere 5. http://dx.doi.org/10.1890/ES13-00391.1 art61.
Shanahan, T.M., McKay, N.P., Hughen, K.A., Overpeck, J.T., Otto-Bliesner, B., Heil, C.W., King, J., Scholz, C.A., Peck, J., 2015. The time-transgressive termination of the African Humid period. Nat. Geosci. 8, 140–144. http://dx.doi.org/10.1038/ngeo2329.
Shuman, B., 2012a. Recent Wyoming temperature trends, their drivers, and impacts in a 14,000-year context. Clim. Change 112, 429–447. http://dx.doi.org/10.1007/s10584-011-0223-5.
Shuman, B., 2012b. Patterns, processes, and impacts of abrupt climate change in a warm world: the past 11,700 years. Wiley Interdiscip. Rev. Clim. Change 3, 19–43. http://dx.doi.org/10.1002/wcc.152.
Shuman, B., Huang, Y., Newby, P., Wang, Y., 2006. Compound-specific isotopic analyses track changes in the seasonality of precipitation in the northeastern United States at ca. 8200 cal yr BP. Quat. Sci. Rev. 25, 2992–3002.
Shuman, B.N., Pribyl, P., Buettner, J., 2015. Hydrologic changes in Colorado during the mid-Holocene and Younger Dryas. Quat. Res. 84, 187–199. http://dx.doi.org/10.1016/j.yqres.2015.07.004.
Shuman, B., Pribyl, P., Minckley, T.A., Shinker, J.J., 2010. Rapid hydrologic shifts and prolonged droughts in Rocky Mountain headwaters during the Holocene. Geophys. Res. Lett. 37, L06701. http://dx.doi.org/10.1029/2009gl042196.
Shuman, B.N., Bartlein, P.J., Logar, N., Newby, P., Webb, T., 2002. Parallel climate and vegetation responses to the early Holocene collapse of the Laurentide Ice Sheet. Quat. Sci. Rev. 21, 1793–1805.
Shuman, B.N., Carter, G.E., Hougardy, D.D., Powers, K., Shinker, J.J., 2014. A north–south moisture dipole at multi-century scales in the central and southern Rocky Mountains, U.S.A., during the late Holocene. Rocky Mt. Geol. 49, 33–49. http://dx.doi.org/10.2113/gsrocky.49.1.33.
Shuman, B.N., Newby, P., Huang, Y., Webb, T., 2004. Evidence for the close climatic control of New England vegetation history. Ecology 85, 1297–1310.
Smith, A.J., Donovan, J.J., Ito, E., Engstrom, D.R., Panek, V.A., 2002. Climate-driven hydrologic transients in lake sediment records: multoproxy record of mid-Holocene drought. Quat. Sci. Rev. 21, 625.
Smith, M.A., Hollander, D.J., 1999. Historical linkage between atmospheric circulation patterns and the oxygen isotopic record of sedimentary carbonates from

Lake Mendota, Wisconsin, USA. Geology 27, 589–592. http://dx.doi.org/10.1130/0091-7613(1999)027<0589:hlbacp>2.3.co;2.
Solignac, S., de Vernal, A., Hillaire-Marcel, C., 2004. Holocene sea-surface conditions in the North Atlantic–contrasted trends and regimes in the western and eastern sectors (Labrador Sea vs. Iceland Basin). Quat. Sci. Rev. 23, 319–334.
Spear, R.W., Davis, M.B., Shane, L.C.K., 1994. Lake Quaternary history of low-and mid-elevation vegetation in the White Mountains of New Hampshire. Ecol. Monogr. 64, 85.
Steinman, B.A., Abbott, M.B., 2013. Isotopic and hydrologic responses of small, closed lakes to climate variability: hydroclimate reconstructions from lake sediment oxygen isotope records and mass balance models. Geochim. Cosmochim. Acta 105, 342–359. http://dx.doi.org/10.1016/j.gca.2012.11.027.
Telford, R.J., Birks, H.J.B., 2005. The secret assumption of transfer functions: problems with spatial autocorrelation in evaluating model performance. Quat. Sci. Rev. 24, 2173–2179. http://dx.doi.org/10.1016/j.quascirev.2005.05.001.
Thornalley, D.J.R., Elderfield, H., McCave, I.N., 2009. Holocene oscillations in temperature and salinity of the surface subpolar North Atlantic. Nature 457, 711–714.
Tierney, J.E., deMenocal, P.B., 2013. Abrupt shifts in Horn of Africa hydroclimate since the last glacial maximum. Science 342, 843–846. http://dx.doi.org/10.1126/science.1240411.
Van Geel, B., Heusser, C.J., Renssen, H., Schuurmans, C.J.E., 2000. Climatic change in Chile at around 2700 BP and global evidence for solar forcing: a hypothesis. Holocene 10, 659–664. http://dx.doi.org/10.1191/09596830094908.
Van Zant, K., 1979. Late glacial and postglacial pollen and plant macrofossils from Lake West Okoboji, Northwestern Iowa. Quat. Res. 12, 358–362.
Viau, A.E., Gajewski, K., Sawada, M.C., Fines, P., 2006. Millennial-scale temperature variations in north America during the Holocene. J. Geophys. Res. 111.
Wagner, A.J., Morrill, C., Otto-Bliesner, B.L., Rosenbloom, N., Watkins, K.R., 2013. Model support for forcing of the 8.2 ka event by meltwater from the Hudson Bay ice dome. Clim. Dyn. 41, 2855–2873. http://dx.doi.org/10.1007/s00382-013-1706-z.
Walker, M.J.C., Berkelhammer, M., Björck, S., Cwynar, L.C., Fisher, D.A., Long, A.J., Lowe, J.J., Newnham, R.M., Rasmussen, S.O., Weiss, H., 2012. Formal subdivision of the Holocene series/epoch: a discussion paper by a working group of INTIMATE (integration of ice-core, marine and terrestrial records) and the subcommission on quaternary stratigraphy (international commission on stratigraphy). J. Quat. Sci. 27, 649–659. http://dx.doi.org/10.1002/jqs.2565.
Wanner, H., Beer, J., Bütikofer, J., Crowley, T.J., Cubasch, U., Flückiger, J., Goosse, H., Grosjean, M., Joos, F., Kaplan, J.O., Küttel, M., Müller, S.A., Prentice, I.C., Solomina, O., Stocker, T.F., Tarasov, P., Wagner, M., Widmann, M., 2008. Mid- to Late Holocene climate change: an overview. Quat. Sci. Rev. 27, 1791–1828.
Wanner, H., Solomina, O., Grosjean, M., Ritz, S.P., Jetel, M., 2011. Structure and origin of Holocene cold events. Quat. Sci. Rev. 30, 3109–3123. http://dx.doi.org/10.1016/j.quascirev.2011.07.010.
Watts, W.A., Bright, R.C., 1968. Pollen, seed, and mollusk analysis of a sediment core from Pickerel Lake, northeastern South Dakota. Geol. Soc. Am. Bull. 79, 855–876.
Webb III, T., 1986. Is vegetation in equilibrium with climate? How to interpret late-Quaternary pollen data. Vegetatio 67, 75–91.
Whitmore, J., Gajewski, K., Sawada, M., Williams, J., Shuman, B., Bartlein, P.J., Shafer, S., Minckley, T., Viau, A., Brubaker, L., 2005. An updated modern pollen-climate-vegetation dataset for North America. Quat. Sci. Rev. 24, 1828–1848.
Williams, J.W., Shuman, B., 2008. Obtaining accurate and precise environmental reconstructions from the modern analog technique and North American surface pollen dataset. Quat. Sci. Rev. 27, 669–687.
Williams, J.W., Shuman, B., Bartlein, P.J., Diffenbaugh, N.S., Webb, T., 2010. Rapid, time-transgressive, and variable responses to early Holocene midcontinental drying in North America. Geology 38, 135–138. http://dx.doi.org/10.1130/g30413.1.
Wright Jr., H.E., Stefanova, I., Tian, J., Brown, T.A., Hu, F.S., 2004. A chronological framework for the Holocene vegetational history of central Minnesota: the Steel Lake pollen record. Quat. Sci. Rev. 23, 611–626. http://dx.doi.org/10.1016/j.quascirev.2003.09.003.
Yu, S.-Y., Colman, S.M., Lowell, T.V., Milne, G.A., Fisher, T.G., Breckenridge, A., Boyd, M., Teller, J.T., 2010. Freshwater outburst from lake superior as a trigger for the cold event 9300 Years Ago. Science 328, 1262–1266. http://dx.doi.org/10.1126/science.1187860.
Yu, Z., Andrews, J.H., Eicher, U., 1997. Middle Holocene dry climate caused by change in atmospheric circulation patterns: evidence from lake levels and stable isotopes. Geology 25, 251–254.
Zhao, Y., Yu, Z.C., Zhao, C., 2010. Hemlock (Tsuga canadensis) declines at 9800 and 5300 cal yr BP caused by Holocene climatic shifts in northeastern North America. Holocene 20, 877–886. http://dx.doi.org/10.1177/0959683610365932.